ORGANOMETALLICS

Article

pubs.acs.org/Organometallics

Investigation of the Electronic Origin of Asymmetric Induction in Palladium-Catalyzed Allylic Substitutions with Phosphinooxazoline (PHOX) Ligands by Hammett and Swain–Lupton Analysis of the ^{13}C NMR Chemical Shifts of the (π-Allyl)palladium Intermediates

Paul B. Armstrong, Elizabeth A. Dembicer, Andrew J. DesBois, Jay T. Fitzgerald, Janet K. Gehrmann, Nathaniel C. Nelson, Amelia L. Noble, and Richard C. Bunt*

Department of Chemistry & Biochemistry, Middlebury College, Middlebury, Vermont 05753, United States

Supporting Information

ABSTRACT: Isomeric 4′- and 5′-substituted phosphinooxazoline (PHOX) ligands are used to probe the electronic origins of enantioselective nucleophilic additions to (1,3-diphenylallyl)palladium PHOX ligand complexes. Hammett analysis of the ^{13}C NMR chemical shifts of the allyl C-1 and C-3 carbons shows that the major exo diastereomer is less susceptible to differential changes at C-1 and C-3 and that the location of the substituent has a smaller impact on these changes. In contrast, the minor endo diastereomer is more susceptible to differential ^{13}C NMR changes at C-1 and C-3 and the location of the substituent has a greater impact on these changes. The endo diastereomer exhibits a pronounced "cis effect" by the ligating nitrogen and phosphorus atoms across the palladium center that explains its lower reactivity and, therefore, how the enantioselectivity typically obtained with PHOX ligands exceeds the approximately 8/1 ratio of exo to endo intermediates. Swain–Lupton analysis reveals the importance of both resonance and field effects by the substituents regardless of their location and supports the overall electronic control model for enantioselection by PHOX ligands. For rational chiral ligand design and electronic tuning of ligand properties, these results suggest that the overall electronic impact of a remote substituent generally depends more on its identity than on its location within the ligand.

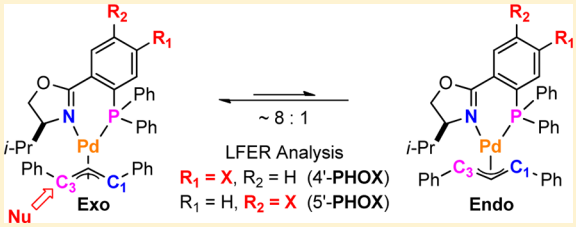

INTRODUCTION

The phosphinooxazoline (PHOX) ligands **1** introduced by Helmchen, Pflatz, and Williams in 1993[1] have proven to be one of the most effective non-C_2-symmetric ligand classes for palladium-catalyzed allylic substitutions.[2−4] These ligands are understood to function both sterically, by controlling the ratio of the exo to endo (π-allyl)palladium intermediates **4**, as well as electronically, by directing nucleophilic addition trans to phosphorus (the better acceptor ligand)[5] in the favored exo diastereomer.[6] In particular, the low-temperature NMR structure of the initially formed (alkene)palladium(0) product complex established the major nucleophilic addition pathway as trans to phosphorus in the exo diastereomer,[7] but it did not provide any information about the pathway(s) leading to the minor enantiomer or the role of the minor endo diastereomer in determining the level of enantioselectivity. Furthermore, despite the success and intuitive appeal of electronically based stereocontrol in these systems, steric effects still predominate in many mixed donor ligands in which a strong electronic trans effect would have been expected.[8] Our previous Hammett studies of the reaction enantioselectivity with 4′-substituted PHOX ligands **2**[9] and the ^{13}C NMR chemical shifts and X-ray structures of (π-allyl)palladium intermediates **5**[10] provided direct support for the electronic, rather than steric, basis for this regiocontrol in the nucleophilic addition step. Nevertheless, because electronic tuning is a widely used strategy in chiral ligand design,[11] it is important to understand how the electronic effects are transmitted from the ligand to the reactive center(s) and how they impact both the major and the minor nucleophilic addition pathways. To address these issues, we expanded our set of 4′-substituted PHOX ligands (**2a−f**, 4′-PHOX), synthesized isomeric 5′-substituted PHOX ligands (**3a−f**, 5′-PHOX), prepared the corresponding (π-allyl)-palladium complexes (**5a−f** and **6a−f**), and studied the ^{13}C NMR chemical shifts of the allyl C-1 and C-3 carbons by two different linear free energy relationship (LFER)[12] methods—single-parameter Hammett analysis and dual-parameter Swain–Lupton analysis.

Analysis of LFERs has proven useful for understanding a number of transition-metal-catalyzed reactions,[13] and ^{13}C NMR chemical shifts, though not a direct measure of electron density, have been correlated both to positive charge density and to the regioselectivity of nucleophilic attack on (π-allyl)palladium complexes.[14] With achiral ligands, Hammett analysis has been used to successfully correlate the ^{13}C NMR chemical shifts of substituted (π-allyl)palladium complexes to the regiochemistry of nucleophilic attack.[15] More broadly, ^{13}C NMR chemical

Received: July 27, 2012
Published: September 14, 2012

   dx.doi.org/10.1021/om3007163 | *Organometallics* 2012, 31, 6933−6946

Scheme 1. Ligand Synthesis Routes

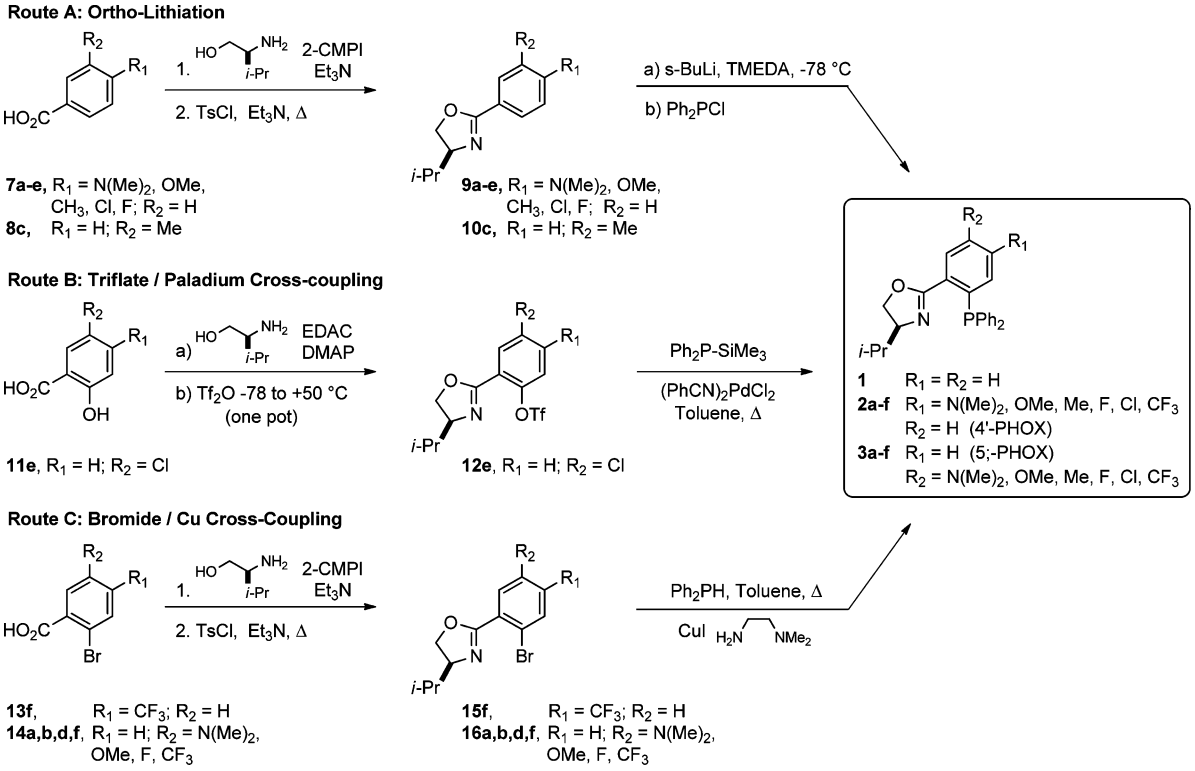

shifts have been correlated by LFERs in a variety of systems.[16,17] In many instances, ^{13}C NMR chemical shifts have been found to correlate better with dual-parameter Swain–Lupton analysis than with single-parameter Hammett analysis or other dual-parameter methods.[18] Although the Swain–Lupton field (F) and resonance (R) parameters may not perfectly separate out field and resonance components,[12c,19] the F and R parameters are nearly orthogonal to one another as regression constants.[20]

In studying the isomeric 4′- and 5′-PHOX ligand complexes, our primary hypothesis was that the change in location of the substituent relative to both nitrogen (via the oxazoline ring) and phosphorus would allow us to determine if the substituent effects are transmitted more via one ligating atom than the other. In the 4′-PHOX ligands (**2a–f**) the substituents are meta to phosphorus and para to nitrogen, but in the 5′-PHOX ligands (**3a–f**) they are meta to nitrogen and para to phosphorus. Comparative Hammett fits employing either σ_m for the 4′-PHOX ligands and σ_p for the 5′-PHOX ligands or σ_p for the 4′-PHOX ligands and σ_m for the 5′-PHOX ligands should indicate whether nitrogen or phosphorus more effectively transmits the substituent effects through palladium. These effects would then have an impact on the allyl C-1 and C-3 carbons where the nucleophilic addition takes place, presumably via the trans effect.[21] In this manner, the differential roles of nitrogen and phosphorus in controlling the enantioselectivity obtained with PHOX ligands can be distinguished. This goal was only partially realized, as the exo diastereomers did not show dramatically different ^{13}C NMR data or Hammett plots. Analysis of the endo diastereomers, however, was much more differential in terms of both ^{13}C NMR data and Hammett plots. The Hammett analysis also revealed a pronounced "cis effect" for the endo diastereomer. Finally, Swain–Lupton analysis of the substituent effects revealed that the field contribution is much larger than the resonance contribution and that the location of the substituent is less important than its identity.

RESULTS AND DISCUSSION

Ligand Synthesis. Most of the 4′-PHOX ligands were prepared in a manner similar to the original synthesis of the parent PHOX ligand **1**[22] (Scheme 1, route A). Coupling of commercially available 4-substituted benzoic acids **7a–e** and (*S*)-2-amino-3-methyl-1-butanol with Mukiayama's reagent[23] and ring closure with tosyl chloride[24] provided oxazolines **9a–e**. Directed ortho lithiation[25] and reaction with chlorodiphenylphosphine[2a] provided ligands **2a–e**. The 5′-methyl-substituted ligand **3c** was also prepared by this route. The regioselectivity of the lithiation and phosphine addition was confirmed by analysis of the ^{1}H NMR aromatic coupling patterns, which showed the 2′-hydrogen in **10c** had been replaced by the diphenylphosphino group in **3c** and that the isolated 6′-hydrogen remained.

Synthesis of the 5′-PHOX ligands was initially envisioned starting from the commercially available 5-substituted salicylic acids employing a palladium-catalyzed cross-coupling of the aryl triflate with (trimethylsilyl)diphenylphosphine[26] (Scheme 1, route B). We developed a convenient protocol that coupled the salicylic acid to (*S*)-2-amino-3-methyl-1-butanol, closed the oxazoline ring, and made the aryl triflate in a single pot. Although we prepared several other aryl-substituted triflates by this route (R_2 = OMe, Me, F), only the chloro derivative **12e** successfully cross-coupled to give ligand **3e**. A number of other palladium and nickel catalyst/diphenylphosphine combinations[27] were tried without success in our hands. These attempts all resulted in either recovered starting material or decomposition. Ultimately, we employed the more recent Stoltz *t*-BuPHOX synthesis protocol[11e] using Buchwald's copper-

dx.doi.org/10.1021/om3007163 | *Organometallics* 2012, 31, 6933–6946

catalyzed cross-coupling[28] to prepare most of the 5′-PHOX ligands (Scheme 1, route C). Formation of oxazolines **15f** and **16a,b,d,f** proceeded as before from the 4- or 5-substituted 2-bromobenzoic acids,[29] and these underwent cross-coupling with diphenylphosphine to give both ligand **2f**, which could not be prepared by route A due to rapid decomposition under the isolation conditions following ortho lithiation/coupling, and ligands **3a,b,d,f**. Thus, by multiple routes we had access to a variety of 4′- and 5′-substituted PHOX ligands (**2a−f** and **3a−f**).

(π-Allyl)palladium Complex Formation and NMR Assignments. Complexes **4**, **5a−f**, and **6a−f** (Chart 1) were

Chart 1. Exo and Endo (π-Allyl)palladium Complexes

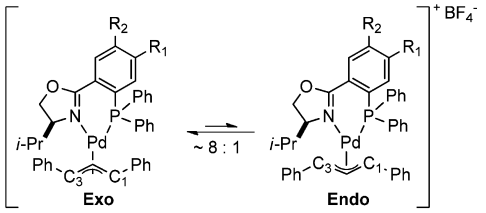

4 $R_1 = R_2 = H$
5a-f $R_1 = N(Me)_2$, OMe, Me, F, Cl, CF_3; $R_2 = H$
6a-f $R_1 = H$; $R_2 = N(Me)_2$, OMe, Me, F, Cl, CF_3

prepared from the corresponding ligand and (1,3-diphenylallyl)palladium chloride dimer by reaction with silver tetrafluoroborate in acetone.[15c] Filtration and removal of the solvent gave the complexes in essentially quantitative yield and with sufficient purity for NMR spectroscopy. Complexes **4**[6b,30] and **5a−e**[10] have been previously reported and characterized, but they were reprepared for direct comparison with complexes **5f** and **6a−f** in this investigation.[31] Although stable for days to weeks in solution, all the complexes were prepared immediately prior to acquiring the NMR data. All NMR spectra were taken in CD_2Cl_2 and referenced relative to the center line of the CD_2Cl_2 pentet at 55.00 ppm.

The ^1H and ^{13}C NMR assignments for the exo and endo diastereomers were tentatively made on the basis of analogy with the literature data for complex **4**, which has been established to exist predominantly in the exo conformation in solution.[31] To confirm the NMR assignments for each of the complexes in this study, a COSY spectrum was taken to identify the H-1 and H-3 allyl hydrogens for both the exo and endo diastereomers by their coupling to H-2. This ^1H chemical shift information was then used to identify the corresponding ^{13}C signals in the HMQC spectrum (see the Supporting Information for sample 2D NMR spectra of **5d**). Finally, a ^{13}C NMR spectrum was used to obtain the chemical shift values reported and was used in the following LFER analyses.

^{13}C NMR Chemical Shift Data and Exo/Endo Ratios. The ^{13}C NMR chemical shifts of allyl carbons C-1 and C-3 in both the exo and endo diastereomers move downfield as the substituents become more electron withdrawing (**a** → **f**) for both **5a−f** (Table 1) and **6a−f** (Table 2). Two trends are of note: (1) the range of chemical shifts as the substituents change (**a** → **f**) and (2) the difference in chemical shifts due to the location of the substituent (4′-PHOX vs 5′-PHOX). For the exo diastereomers the ranges of chemical shift changes for **5a−f** and **6a−f** at C-1 and C-3 are quite similar (1.75 and 1.94 ppm at C-1; 1.48 and 1.50 ppm at C-3). In contrast, for the endo diastereomer the range for **5a−f** is larger at C-3 than that at C-1

Table 1. ^{13}C NMR Chemical Shifts[a] of (π-Allyl)palladium Complexes 5a−f (4′-PHOX)

complex	substituent	C-1 (exo)	C-3 (exo)	C-1 (endo)	C-3 (endo)
5a	NMe_2	70.10	100.30	74.31	94.42
5b	OMe	70.80	101.06	74.96	95.27
5c	Me	70.81	101.06	74.85	95.40
4	H	70.98	101.11	75.02	95.56
5d	F	71.48	101.56	75.62	96.01
5e	Cl	71.54	101.64	75.62	96.12
5f	CF_3	71.85	101.78	75.82	96.62
range	**a** → **f**	1.75	1.48	1.51	2.20

[a]All chemical shifts are reported in ppm relative to the center line of the CD_2Cl_2 pentet at 55.00 ppm.

Table 2. ^{13}C NMR Chemical Shifts[a] of (π-Allyl)palladium Complexes 6a−f (5′-PHOX)

complex	substituent	C-1 (exo)	C-3 (exo)	C-1 (endo)	C-3 (endo)
6a	NMe_2	69.98	100.39	73.78	94.85
6b	OMe	70.70	100.92	74.61	95.43
6c	Me	70.82	101.03	74.80	95.48
4	H	70.98	101.11	75.02	95.56
6d	F	71.41	101.53	75.41	96.09
6e	Cl	71.51	101.64	75.58	96.06
6f	CF_3	71.92	101.89	76.11	96.39
range	**a** → **f**	1.94	1.50	2.33	1.54

[a]All chemical shifts are reported in ppm relative to the center line of the CD_2Cl_2 pentet at 55.00 ppm.

(2.20 ppm vs 1.51 ppm) and for **6a−f** it is larger at C-1 than at C-3 (2.33 ppm vs 1.54 ppm). This reversal of which carbon exhibits the larger range of chemical shifts for the endo diastereomer indicates that the substituent at the 4′-position (**5a−f**) has a greater effect on C-3 (trans to phosphorus) and the substituent at the 5′-position (**6a−f**) has a greater effect on C-1 (trans to nitrogen). Second, the differences in chemical shift between the 4′-PHOX and 5′-PHOX isomers for any given substituent vary but are generally much larger for the endo diastereomers than for the exo diastereomers. The absolute differences in chemical shifts due to the location of the substituent vary from 0.00 ppm (**5e** vs **6e**, C-3 exo) to 0.53 ppm (**5a** vs **6a**, C-1 endo). However, for the exo diastereomers the average absolute difference in chemical shifts at both C-1 and C-3 is 0.07 ppm (**5a−f** vs **6a−f**), but for the endo diastereomer the average absolute difference in chemical shift at C-1 is 0.25 ppm and at C-3 is 0.17 ppm (**5a−f** vs **6a−f**). These two different trends in the ^{13}C NMR chemical shift data both show that the endo diastereomer is more affected by the identity and location of the substituent than the exo diastereomer. Hammett analysis (see below) provides further insight into this differential behavior of the endo diastereomer.

The difference in ^{13}C chemical shift ($\Delta\delta$) between C-3 and C-1 in (π-allyl)palladium complexes has been related to the overall enantioselectivity of the ligand.[32] These differences for **5a−f** and **6a−f** are reported in Table 3. Overall, the exo diastereomers show a larger $\Delta\delta$ (~30.1 ppm) than the endo diastereomers (~20.5 ppm). Neither $\Delta\delta$ changes that much with the identity of the substituent (**a** → **f**), though for most of the complexes the $\Delta\delta$ value gets slightly smaller for more electron withdrawing substituents. The larger $\Delta\delta$ for the exo diastereomer has been reported in (1,3-dialkylallyl)palladium complexes of **1** and related ligands.[6c] The smaller $\Delta\delta$ value for

dx.doi.org/10.1021/om3007163 | Organometallics 2012, 31, 6933−6946

Table 3. Changes in Chemical Shifts ($\Delta\delta^a$ and $\Delta(\Delta\delta)^b$) for (π-Allyl)palladium Complexes

	4, 5a–f (4′-PHOX)		4, 6a–f (5′-PHOX)			
substituent	$\Delta\delta$ (exo)	$\Delta\delta$ (endo)	$\Delta\delta$ (exo)	$\Delta\delta$ (endo)	$\Delta(\Delta\delta)$ (exo)	$\Delta(\Delta\delta)$ (endo)
NMe_2	30.20	20.11	30.41	21.07	+0.21	+0.96
OMe	30.26	20.31	30.22	20.82	−0.04	+0.51
Me	30.25	20.55	30.21	20.68	−0.04	+0.13
H	30.13	20.54	30.13	20.54		
F	30.08	20.39	30.12	20.68	+0.04	+0.29
Cl	30.10	20.50	30.13	20.48	+0.03	−0.02
CF_3	29.93	20.80	29.97	20.28	+0.04	−0.52

$^a\Delta\delta = \delta$(C-3) − δ(C-1). $^b\Delta(\Delta\delta) = \Delta\delta$(**6a–f**) − $\Delta\delta$(**5a–f**).

Table 4. Exo/Endo Ratios[a] for (π-Allyl)palladium Complexes

	exo/endo	
substituent	4, 5a–f (4′-PHOX)	4, 6a–f (5′-PHOX)
NMe_2	89/11	90/10
OMe	90/10	91/9
Me	88/12	90/10
H	90/10	90/10
F	90/10	87/13
Cl	89/11	90/10
CF_3	89/11	90/10

[a]Determined by integration of the allyl H-3 signals at δ 5.8–6.0 ppm (exo) and δ 5.5–5.7 ppm (endo) in the corresponding ^{1}H NMR spectra.

the endo complexes in comparison to that for the exo complexes is likely one of the major reasons that the enantioselectivity obtained with PHOX ligands, often 95–99+ % ee, can greatly exceed the typical 8/1 ratio of exo to endo intermediates.[2,10] The endo diastereomer must be either less reactive or less selective than the exo diastereomer—lower reactivity or selectivity for nucleophilic addition trans to phosphorus by the endo diastereomer would lead to less formation of the minor enantiomer. Experiments with unsymmetrical π-allyl substrates and PHOX ligands have shown that the preference for nucleophilic addition trans to phosphorus is very high (>10^4).[6b] This strong preference suggests that the difference that allows high enantioselectivity with PHOX ligands is primarily the lower reactivity of the endo diastereomer.

As with the chemical shift data itself, the effect of the position of the substituent (4′ vs 5′) can also be seen in the $\Delta\delta$ data. The $\Delta\delta$ differences between **5a–f** and **6a–f** are much smaller for the exo diastereomers than for the endo diastereomers. Subtracting the $\Delta\delta$ for **6a–f** from $\Delta\delta$ for **5a–f**, this $\Delta(\Delta\delta)$ ranges from +0.21 ppm to −0.04 ppm for the exo complex but ranges from +0.96 ppm to −0.52 ppm for the endo complex (Table 3). For the endo diastereomer electron-donating groups at the 5′-position increase the chemical shift difference between C-3 and C-1 ($\Delta\delta$) and electron-withdrawing groups at the 5′-position, $-CF_3$ in particular, reduce it. These $\Delta(\Delta\delta)$ trends provide a different way of viewing the differing overall ranges and the individual changes in chemical shifts due to the position of the substituent discussed previously. The $\Delta(\Delta\delta)$ trends also make it easier to see that the endo diastereomers vary more consistently with the nature of the substituent (**a** → **f**) than the exo diastereomers in a way that relates directly to the reactivity of the complex.

To determine if these substituent effects have an impact on the relative stability of the exo and endo diastereomers, the exo/endo ratio for all of the complexes was determined by integration of the allyl H-3 signals in the ^{1}H NMR spectrum (Table 4). This signal was used because it is uniformly distinct and free from any other overlapping signals for all of the complexes. The exo/endo ratio is fairly constant around 8/1 to 9/1 for all of the complexes in CD_2Cl_2 and shows no clear trends with the changing substituents (**a** → **f**). Thus, the favorability of the exo (π-allyl)palladium intermediate does seem predominantly steric in nature or is at least unaffected by these electronic perturbations to the ligand. The exo/endo ratio has shown some solvent dependence and has been reported for similar PHOX ligand (1,3-diphenylallyl)palladium complexes as 8/1 in THF-d_8, 11/1 in DMSO-d_6, and 6/1 in $CDCl_3$.[2,33]

Hammett Analysis of ^{13}C NMR Data. On the basis of our hypothesis that the differing backbone locations of the substituents on the PHOX ligand (i.e., **5a–f** vs **6a–f**) would provide insight into the manner that the electronic influences of nitrogen and phosphorus are transmitted from the ligand through palladium to the π-allyl fragment, we carried out Hammett analysis of the ^{13}C NMR data from Tables 1 and 2 with least-squares linear regression. To compare the effect via nitrogen or phosphorus, we employed either σ_m for **5a–f** and σ_p for **6a–f** (Figure 1) or σ_p for **5a–f** and σ_m for **6a–f** (Figure 2). The rationale for these two methods is that in **5a–f** the substituents are meta to phosphorus and para to nitrogen (via the oxazoline ring) and in **6a–f** the substituents are para to phosphorus and meta to nitrogen. Thus, either σ_m or σ_p could be the "correct" parameter to employ for either ligand isomer if either nitrogen (trans to C-1) or phosphorus (trans to C-3) has a dominant effect. These two limiting scenarios would be distinguished by better correlating Hammett plots in Figure 1 if the effects via phosphorus (meta to the substituent in **5a–f** and para in **6a–f**) dominate or Figure 2 if the effects via nitrogen (para to the substituent in **5a–f** and meta in **6a–f**) dominate.

For all of the Hammett plots the slopes are positive, reflecting the downfield chemical shifts as the substituents become more electron withdrawing, and vary from +1.20 to +1.73 in magnitude. For the exo diastereomers (solid symbols and lines), the goodness of the linear data fits does not differ that much with either version of the Hammett plot (Figure 1 vs Figure 2). The R^2 values range from 0.72 to 0.81 for all four of the exo Hammett plots. This outcome suggests that the electronic influences via nitrogen and phosphorus are both important and cannot be so easily separated. However, for the endo diastereomers (open symbols and dashed lines) the C-1 Hammett plot in Figure 1b with σ_m for **5a–f** and σ_p for **6a–f** (substituent positions relative to phosphorus) is much better (R^2 = 0.91 vs R^2 = 0.56) than the corresponding C-1 Hammett plot in Figure 2b (substituent positions relative to nitrogen). In contrast, the C-3 endo Hammett plot in Figure 2a with σ_p for **5a–f** and σ_m for **6a–f** (substituent positions relative to nitrogen) is much better (R^2 = 0.87 vs R^2 = 0.62) than the corresponding C-3 endo Hammett plot in Figure 1a (substituent positions relative to phosphorus). Furthermore, the slopes for these two better-fitting endo Hammett plots are the largest of all the Hammett plots at +1.73 and +1.59, respectively. The better correlations for these two Hammett plots imply that for the endo diastereomer the dominant effect

dx.doi.org/10.1021/om3007163 | Organometallics 2012, 31, 6933–6946

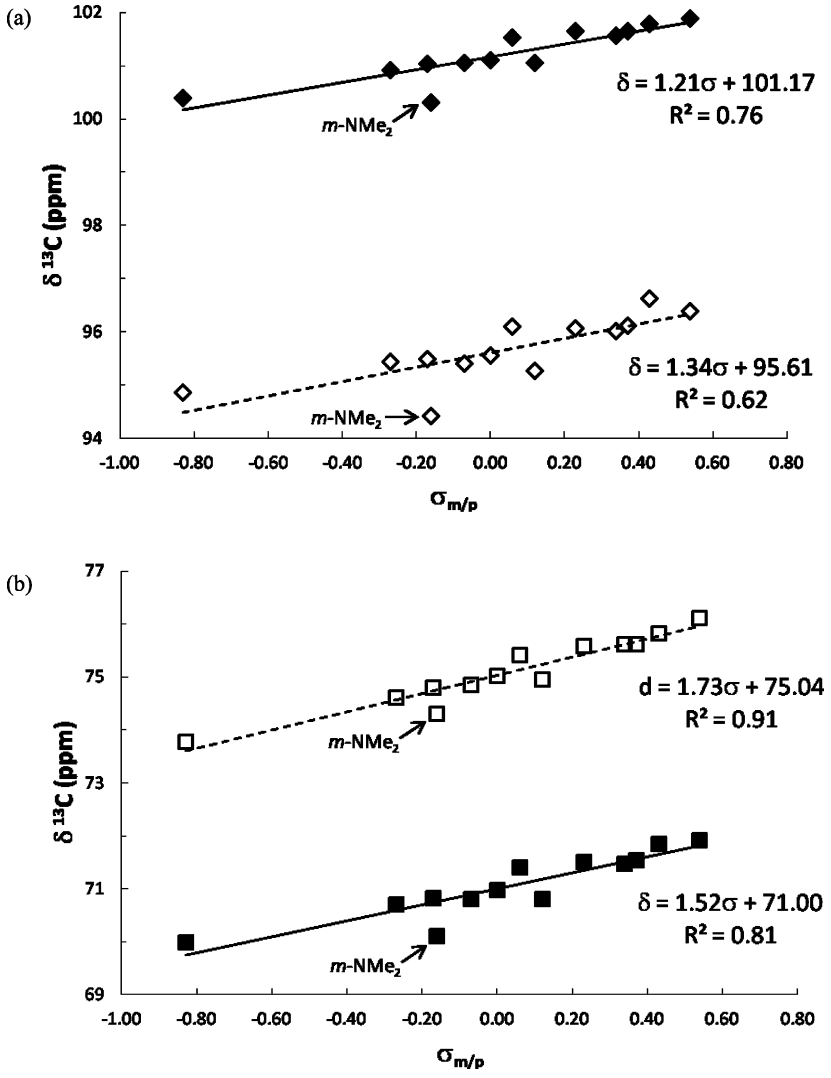

Figure 1. Hammett plots of $\delta(^{13}C)$ vs σ_m for **5a**−**f** and σ_p for **6a**−**f**, with substituent positions relative to phosphorus: (a) C-3 exo (◆) and C-3 endo (◇); (b) C-1 endo (□) and C-1 exo (■).

on C-1 occurs via phosphorus and the dominant effect on C-3 occurs via nitrogen, both cis to one another relative to the palladium center. This combination of phosphorus affecting C-1 to produce a downfield change in chemical shift and nitrogen affecting C-3 to produce an upfield change in chemical shift partially offsets the normal trans effect of phosphorus in the endo diastereomer that causes the chemical shift of C-3 to be downfield of C-1 in both diastereomers in the first place.

A "cis effect", or diminished trans effect, in the endo diastereomer is not that surprising, considering the steric factors that influence the exo/endo ratio in the first place. Unfavorable interactions between the allyl phenyl group and the equatorial-like phenyl ring on phosphorus disfavor the endo diastereomer relative to the exo diastereomer, where these interactions are minimized.[2] In palladium complexes of PHOX ligands with an unsubstituted allyl ligand (π-C_3H_5) lacking these steric interactions, the endo diastereomer is actually favored (55−60%) in solution and the solid state. The endo diastereomer also shows a greater $\Delta\delta$ value in the ^{13}C NMR shifts than the minor exo diastereomer (24 ppm vs 18 ppm).[34] On the basis of these observations, it is the steric interactions between the ligand and the allyl group that dictate how well and in what manner the electronic influences of the ligand are transmitted across the palladium center to the allyl C-1 and C-3 carbons in each diastereomer. In the 1,3-diphenylallyl complexes **4**−**6**, both the minor endo diastereomer is more sensitive to electronic perturbations overall and the allyl C-1 and C-3 carbons are influenced by the cis ligating atom more than they are in the exo diastereomer. Consequently, the "cis effect" in the endo diastereomer explains its smaller $\Delta\delta$ and therefore its lower reactivity than the exo complex.

One of the most notable outliers on all the Hammett plots is the *m*-NMe_2 group (labeled in Figures 1 and 2). In fact, if this single data point is removed from the analysis, the R^2 values get dramatically better for all the Hammett plots (Figures S1 and S2, Supporting Information). The overall similarities for the exo complexes and differences for the endo complexes, however, remain as previously described. Removing this data point is not claimed to be supported on statistical grounds but merely shows that it contributes a great deal to the scatter in the data. The −0.16 value of σ_m for $-NMe_2$ seems to poorly represent the impact of the substituent on the chemical shift. In fact, complexes **5a** and **6a** exhibit the most upfield chemical shifts at C-1 and C-3 in both the exo and endo diastereomers. For $-NMe_2$, the σ_m value reflects more of the inductive electron-withdrawing nature of the group, and clearly the resonance

dx.doi.org/10.1021/om3007163 | *Organometallics* 2012, 31, 6933−6946

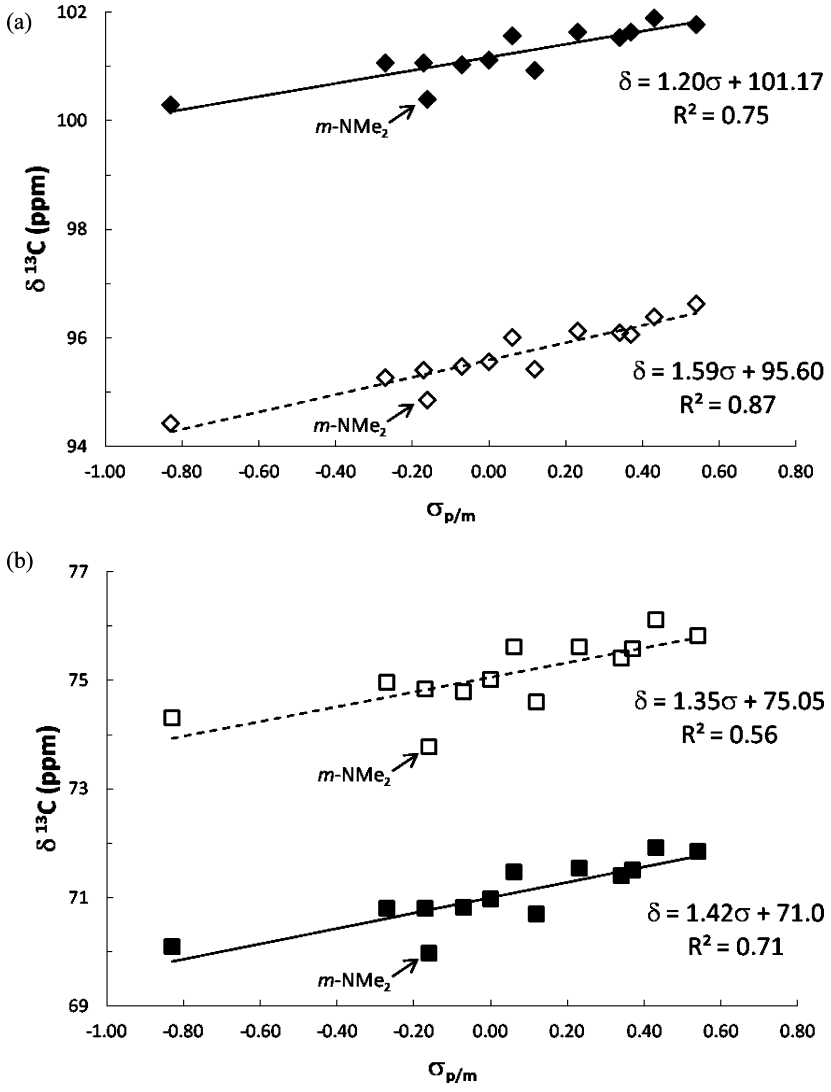

Figure 2. Hammett plots of $\delta(^{13}C)$ vs σ_p for **5a–f** and σ_m for **6a–f**, with substituent positions relative to nitrogen: (a) C-3 exo (◆) and C-3 endo (◇); (b) C-1 endo (□) and C-1 exo (■).

donation of the $-NMe_2$ group is important regardless of its position relative to nitrogen and phosphorus. In fact, this type of impact is more general than just the $-NMe_2$ group. In separate Hammett plots of the data for complexes **5a–f** and **6a–f**, each versus σ_m or σ_p, both ligand series fit σ_p better than σ_m. (Figures S3–S6, Supporting Information). This outcome not only supports the importance of resonance effects, as σ_p is known to have a strong resonance component,[12] but also suggests that Swain–Lupton field and resonance dual-parameter analysis might be effective.

Swain–Lupton Analysis of ^{13}C NMR Data. Dual-parameter regression analysis ($\delta = f{\cdot}F + r{\cdot}R$) of the ^{13}C NMR chemical shift data from Tables 1 and 2 was carried out with the modified Swain–Lupton parameters that Hansch recalculated[12a,20] to scale directly with Hammett's original σ constants. The values for the f and r parameters for all eight equations are shown in Table 5. Unlike Hammett's σ constants, the F and R parameters do not depend on position; consequently, the data for **5a–f** and **6a–f** were analyzed separately. In all cases the correlations are very good ($R^2 \geq 0.97$). Although the separate Hammett plots for **5a–f** and **6a–f** (Figures S3–S6, Supporting Information) showed much better correlations with σ_p, which suggested the importance of resonance contributions, the field parameter coefficient (f) is significantly larger (average of 62% relative contribution) than the resonance parameter coefficient (r) for all eight equations. However, this result is not contradictory, as it shows that the resonance component of each substituent has about the same impact (average of 38% relative contribution) regardless of its

Table 5. Swain–Lupton Dual-Parameter Fits[a] of ^{13}C NMR Data vs Field (F) and Resonance (R) Parameters

			f	% f	r	% r	R^2
4, 5a-f	exo	C-1	1.99	63	1.15	37	0.99
		C-3	1.66	63	0.98	37	0.97
	endo	C-1	2.05	68	0.94	32	0.99
		C-3	2.12	59	1.49	41	0.99
4, 6a-f	exo	C-1	1.95	60	1.32	40	0.99
		C-3	1.66	62	1.01	38	0.98
	endo	C-1	2.16	57	1.62	43	0.99
		C-3	1.79	64	0.99	36	0.98
average			*1.92*	*62*	*1.19*	*38*	

[a] $\delta = f{\cdot}F + r{\cdot}R$. Values for F and R are taken from ref 12a.

dx.doi.org/10.1021/om3007163 | *Organometallics* 2012, 31, 6933–6946

location. In addition, this result agrees with the broad observation that the location of the substituent (**5a**−**f** vs **6a**−**f**) does not have a large impact on the ^{13}C NMR chemical shifts of the complexes, particularly for the exo diastereomers. The larger field component also makes sense, considering the similar chemical shift data trends for **5a**−**f** and **6a**−**f** as well as the "cis effect" for the endo diastereomer. Thus, the Swain−Lupton treatment explains the data for the exo diastereomers, which did not correlate as well with σ_m and σ_p by either of our previous methods, as well as the data for the endo diastereomers in a consistent fashion.

To provide a more visual assessment of the Swain−Lupton analysis and to compare the exo and endo diastereomers more directly, the average values of f (62%) and r (38%) were used to calculate composite $\sigma_{S\text{-}L}$ constants for each substituent from the F and R parameters ($\sigma_{S\text{-}L} = 0.62F + 0.38R$) (Table 6).[34] With

Table 6. Calculated $\sigma_{S\text{-}L}$ Values from Swain−Lupton Analysis

substituent	$\sigma_{S\text{-}L}$[a]
NMe_2	−0.279
OMe	−0.0330
Me	−0.0622
H	0.0186
F	0.130
Cl	0.188
CF_3	0.296

[a]Calculated by the equation $\sigma_{S\text{-}L} = 0.62F + 0.38R$ (the average values of f and r from Table 5) and the values of F and R taken from ref 12b.

these $\sigma_{S\text{-}L}$ values, the ^{13}C NMR chemical shift data can now be plotted like a single-parameter LFER. Because the $\sigma_{S\text{-}L}$ values, like F and R, are independent of position (meta vs para), the two sets of data (**5a**−**f** and **6a**−**f**) were graphed separately (Figures 3 and 4). In all cases the correlations are very good ($R^2 \geq 0.97$). The success of this $\sigma_{S\text{-}L}$ single-parameter approach is due to the very similar field and resonance contributions to all of the ^{13}C NMR chemical shift changes. Moreover, the $\sigma_{S\text{-}L}$ plots provide a very good graphical impression of how well all the ^{13}C NMR data are treated with the Swain−Lupton approach in comparison to the treatment with single-parameter Hammett analysis (Figures 1 and 2). In addition, the slopes of the best-fit lines provide a simple measure of the relative sensitivity of the ^{13}C NMR data to the electronic perturbations—something much harder to gauge from the dual-parameter regression in Table 5. With one exception (C-1 for **5a**−**f**), the slopes of the endo plots are larger than the slopes for the exo plots for the same carbon. This outcome more graphically shows that the endo complexes are more sensitive to electronic perturbations than the exo complexes, as seen before in the $\Delta(\Delta\delta)$ data and the Hammett plots (Figures 1 and 2, with the same exception for C-1 in Figure 2). In addition, the slopes of all the Hammett plots versus $\sigma_{S\text{-}L}$ are much larger in magnitude than the slopes for the original Hammett plots (Figures 1 and 2). Primarily, this increased slope is a consequence of the compressed range of $\sigma_{S\text{-}L}$ values (−0.279 to +0.296, **a** → **f**). Nonetheless, by taking into account the dual field and resonance properties of the substituents in a single parameter with the same fixed proportions of F and R for all of the substituents, the magnitude of the electronic effects (i.e., the slope) and the goodness of the fits both increase dramatically. Overall, the Swain−Lupton analysis provides a more comprehensive treatment of the electronic effects for both the exo and endo diastereomers. Furthermore, it shows that the transmission of electronic effects via both nitrogen and phosphorus is important and does not depend very much on the position of the substituent relative to nitrogen and phosphorus.

CONCLUSIONS

The results of Hammett and Swain−Lupton analysis work together to provide complementary information about how electronic effects influence enantioselectivity in palladium-catalyzed π-allyl additions with PHOX ligands. Although much is made of the favorability of nucleophilic addition trans to phosphorus in the exo diastereomer for electronic reasons, which these data and analysis supports, it is equally important to the success of the PHOX ligands that nucleophilic addition trans to phosphorus in the endo diastereomer is suppressed. The endo diastereomer is actually more sensitive to electronic effects than the exo diastereomer and exhibits a stronger "cis effect". The transmission of these influences occurs through both nitrogen and phosphorus via resonance and, more significantly, field effects. The position of the substituent on the ligand (4′ or 5′), though useful in these analyses, does not have a large effect on the overall nature of electronic impact of the substituent. For rational chiral ligand design that involves electronic tuning,[11] these results suggest that the identity of the substituent is much more important than its position. This knowledge should be of great utility to others seeking to synthesize electronically modified ligands to optimize reactivity or selectivity, as it is often much easier to introduce electronic tuning groups at certain ligand locations rather than other locations due to the starting materials available, the nature of the substituents, and the types of reactions employed in the synthesis.

EXPERIMENTAL SECTION

General Procedures. All reactions were carried out under nitrogen or argon, as indicated, in glassware that was oven- or flame-dried unless otherwise noted. THF, dichloromethane, and diethyl ether were dried by passage through activated alumina on a commercial solvent purification system. Hexane and toluene were purchased in anhydrous grade over 4 Å molecular sieves. Copper(I) iodide was purified by continuous extraction (Soxhlet) with THF. Bis(μ-chloro)bis(1,3-diphenyl-η^3-allyl)dipalladium,[15c] and (trimethylsilyl)diphenylphosphine[27b] were prepared by literature methods. 4-(Trifluoromethyl)-2-bromobenzoic acid (**13f**) was purchased from Ivy Chemicals, and 5-(trifluoromethyl)-2-bromobenzoic acid (**14f**) was purchased from Matrix Scientific. All other chemicals were purchased from standard suppliers and used as received unless otherwise noted. IR spectra were obtained by diffuse reflectance. ^1H NMR chemical shifts are reported relative to Me_4Si and referenced to the residual $CHCl_3$ solvent signal at 7.27 ppm or the $CHDCl_2$ solvent signal at 5.32 ppm. ^{13}C NMR chemical shifts are reported relative to Me_4Si and referenced to the center line of the CD_2Cl_2 pentet at 54.00 ppm. ^{13}C NMR spectra of complexes **5a**−**f** and **6a**−**f** were taken at 25 °C at a concentration of approximately 0.1 M. Multiple quantum filtered COSY experiments with gradient filtering were obtained in magnitude mode. HMQC experiments with gradient filtering were obtained in magnitude mode. Oxazolines **9a**−**e**,[9] ligand **1**,[2] and ligands **2a**−**e**[9] have previously been reported and characterized. Complexes **4**[31] and **5a**−**e**[10] have previously been reported and characterized but were reprepared for direct comparison in this study (see the Supporting Information for ^1H, ^{13}C, and ^{31}P NMR data).

5-(Dimethylamino)-2-bromobenzoic Acid (14a).[30] To a 100 mL round-bottom flask was added 1.08 g of 5-amino-2-bromobenzoic acid (5.0 mmol, 1.0 equiv), 2.5 mL of acetic acid, 25.0 mL of methanol, and 405 mg of formaldehyde as a 37 wt % solution in water

dx.doi.org/10.1021/om3007163 | Organometallics 2012, 31, 6933−6946

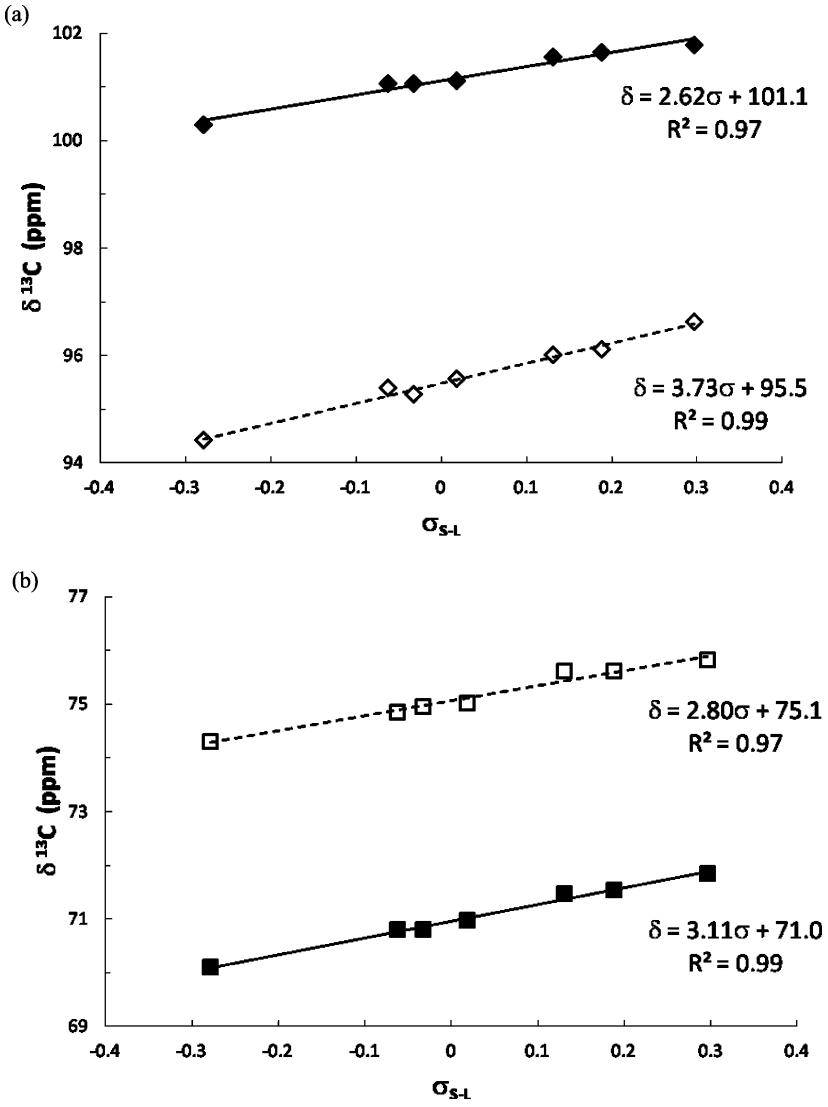

Figure 3. Hammett plots of $\delta(^{13}C)$ vs $\sigma_{S\text{-}L}$ values (from Table 6) for **5a–f**: (a) C-3 exo (◆) and C-3 endo (◇); (b) C-1 endo (□) and C-1 exo (■).

(13.5 mmol, 2.7 equiv). The solution was stirred vigorously and cooled to 0 °C. To the solution was added 943 mg of sodium cyanoborohydride (15.0 mmol, 3 equiv) in three small portions. The reaction mixture was warmed to room temperature and then stirred for an additional 2 h. The solution was concentrated in vacuo, and the product was then diluted with 100 mL of saturated aqueous sodium chloride. The resulting solution was adjusted to pH 6 with saturated aqueous sodium bicarbonate and extracted with ethyl acetate (3 × 50 mL). The combined organic layers were dried over anhydrous sodium sulfate and concentrated in vacuo, to give 1.13 g (92%) of a yellow solid, confirmed by ^{1}H NMR to be sufficiently pure for use in the next step. For analysis, the product was recrystallized from dichloromethane to yield a pale yellow solid, which was then further purified by flash column chromatography (3 cm ×13 cm, 80% ethyl acetate in hexanes). Mp: 149 °C. ^{1}H NMR (400 MHz, $CDCl_3$): δ 9.2 (s, 1 H), 7.5 (d, J = 8.9 Hz, 1 H), 7.3 (d, J = 3.2 Hz, 1 H), 6.7 (dd, J = 8.9, 3.2 Hz, 1 H), 3.0 (s, 6 H). $^{13}C\{^1H\}$ NMR (100 MHz, $CDCl_3$): δ 171.6, 149.3, 134.8, 130.6, 117.2, 115.6, 107.6, 40.4. IR (solid): 2882, 2813, 2385, 1681, 1120, 813 cm^{-1}. Anal. Calcd for $C_9H_{10}BrNO_2$: C, 44.29; H, 4.13; N, 5.74. Found: C, 44.64; H, 4.11; N, 5.80.

General Procedure for Oxazolines 10c, 15f, and 16a,b,d,f. To a round-bottom flask was added (*S*)-(+)-2-amino-3-methyl-1-butanol (1.2 equiv), the substituted benzoic acid (1.0 equiv), 2-chloro-1-methylpyridinium iodide (1.2 equiv), triethylamine (2.4 equiv; distilled), and dichloromethane (0.1 M based on substituted benzoic acid). The reaction mixture was stirred under nitrogen at room temperature for 2 h. The reaction mixture was concentrated in vacuo, and the amide was isolated by flash column chromatography (70% ethyl acetate in hexanes) as a white solid that was used without further purification in the subsequent step.

To a round-bottom flask containing the amide intermediate (1.0 equiv) was added *p*-toluenesulfonic acid (1.1 equiv), triethylamine (5 equiv; distilled), and dichloromethane (0.3 M based on amide). The reaction mixture was heated at reflux under nitrogen for 23 h. Then 0.3 mL of water was added and heating was continued for 1 h. The reaction mixture was cooled to room temperature, diluted with dichloromethane, and washed with water (three portions). The organic layer was dried over anhydrous sodium sulfate and then concentrated in vacuo. The product was isolated by flash column chromatography (10–15% ethyl acetate in hexanes) to give the substituted aryl oxazoline.

(–)-(4S)-4,5-Dihydro-2-(5′-methoxy-2′-bromophenyl)-4-isopropyloxazole (16b). In a 100 mL round-bottom flask was added 248 mg of (*S*)-(+)-2-amino-3-methyl-1-butanol (2.4 mmol, 1.2 equiv), 462 mg of 5-methoxy-2-bromobenzoic acid (**14b**; 2.0 mmol, 1.0 equiv), 613 mg of 2-chloro-1-methylpyridinium iodide (2.4 mmol, 1.2 equiv), 486 mg of triethylamine (4.8 mmol, 2.4 equiv; distilled), and 20.0 mL of dichloromethane. The reaction mixture was stirred under nitrogen at room temperature for 2 h. The reaction mixture was concentrated in vacuo, and the amide was isolated by flash column chromatography (3

dx.doi.org/10.1021/om3007163 | *Organometallics* 2012, 31, 6933–6946

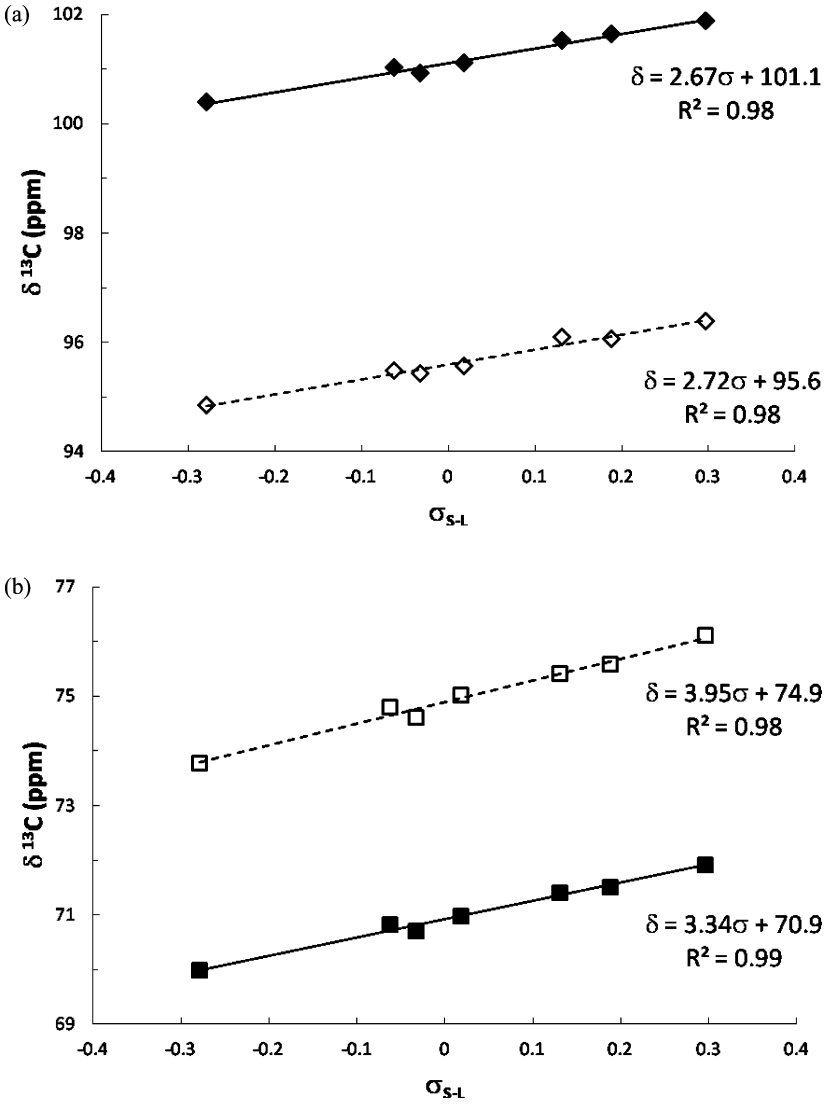

Figure 4. Hammett plots of $\delta(^{13}C)$ vs $\sigma_{S\text{-}L}$ (from Table 6) for **6a–f**: (a) C-3 exo (◆) and C-3 endo (◇); (b) C-1 endo (□) and C-1 exo (■).

cm × 11 cm, 70% ethyl acetate in hexanes) to give 625 mg of a white solid that was used without further purification in the following step. ^{1}H NMR (400 MHz, $CDCl_3$): δ 7.4 (d, J = 8.8 Hz, 1 H), 7.0 (d, J = 3.1 Hz, 1 H), 6.8 (dd, J = 9.2, 3.1 Hz, 1 H), 6.5 (d, J = 8.5 Hz, 1 H), 3.8 (m, 1 H), 3.8 (s, 3 H), 3.7 (m, 2 H), 3.1 (bs, 1 H), 2.0 (m, 1 H), 1.03 (d, J = 2.1 Hz, 3 H), 1.0 (d, J = 2.0 Hz, 3 H).

In a 50 mL round-bottom flask containing 625 mg (2.0 mmol, 1.0 equiv) of the amide was added 419 mg of *p*-toluenesulfonic acid (2.2 mmol, 1.1 equiv), 1.01 g of triethylamine (10.0 mmol, 5 equiv; distilled), and 6.0 mL of dichloromethane. The reaction mixture was heated at reflux under nitrogen for 23 h. Then 0.3 mL of water was added and heating was continued for 1 h. The reaction mixture was cooled to room temperature, diluted with 25 mL of dichloromethane, and washed with water (3 × 10 mL). The organic layer was dried over anhydrous sodium sulfate and then concentrated in vacuo. Flash column chromatography (3 cm × 12 cm, 15% ethyl acetate in hexanes) gave 406 mg (68% overall) of oxazoline **16b** as a clear oil. $[\alpha]_D$ = −48.6° (*c* 1.20, $CHCl_3$). ^{1}H NMR (400 MHz, $CDCl_3$): δ 7.5 (d, J = 8.8 Hz, 1 H), 7.2 (d, J = 3.0 Hz, 1 H), 6.8 (dd, J = 8.8, 3.0 Hz, 1 H), 4.4 (m, 1 H), 4.15 (m, 2 H), 3.78 (s, 3 H), 1.9 (m, 1 H), 1.0 (d, J = 6.8 Hz, 3 H), 0.97 (d, J = 6.7 Hz, 3 H). $^{13}C\{^1H\}$ NMR (100 MHz, $CDCl_3$): δ 162.5, 158.4, 134.3, 130.6, 117.8, 116.1, 111.9, 72.8, 70.2, 55.4, 32.5, 18.6, 18.1. IR (neat): 3051, 2959, 2903, 2873, 1656, 1467, 1223, 1043, 1016, 839, 732 cm^{-1}. Anal. Calcd for $C_{13}H_{16}BrNO_2$: C, 52.36; H, 5.41; N, 4.70. Found: C, 52.51; H, 5.52; N, 4.75.

*(−)-(4S)-4,5-Dihydro-2-(5′-methylphenyl)-4-isopropyloxazole (**10c**).* Following the general procedure, 544 mg of 5-methylbenzoic acid (**8c**; 4.0 mmol) gave 722 mg (89%) of oxazoline **10c** as a clear oil. Data for the amide are as follows. ^{1}H NMR (400 MHz, $CDCl_3$): δ 7.55 (s, 1 H), 7.52 (d, J = 7.1 Hz, 1 H), 7.2 (m, 2 H), 6.8 (d, J = 8.7 Hz, 1 H), 3.9 (m, 1 H), 3.8 (bs, 1 H), 3.7 (m, 2 H), 2.3 (s, 3 H), 2.0 (m, 1 H), 0.95 (m, 6 H). Data for the oxazoline are as follows. $[\alpha]_D$ = −77.1° (*c* 2.47, $CHCl_3$). ^{1}H NMR (400 MHz, $CDCl_3$): δ 7.9 (m, 1 H), 7.8 (m, 1 H), 7.35 (m, 2 H), 4.5 (m, 1 H), 4.2 (m, 2 H), 2.4 (s, 3 H), 1.95 (m, 1 H), 1.05 (d, J = 6.8 Hz, 3 H), 0.96 (d, J = 6.8 Hz, 3 H). $^{13}C\{^1H\}$ NMR (100 MHz, $CDCl_3$): δ 163.4, 137.8, 131.8, 128.7, 128.0, 127.6, 125.2, 72.3, 69.9, 32.6, 21.1, 18.8, 17.9. IR (neat): 2958, 2900, 1650, 1353, 969, 709 cm^{-1}. Anal. Calcd for $C_{13}H_{17}NO$: C, 76.81; H, 8.43; N, 6.89. Found: C, 76.60 ; H, 8.52; N, 7.01.

*(−)-(4S)-4,5-Dihydro-2-(4′-(trifluoromethyl)-2′-bromophenyl)-4-isopropyloxazole (**15f**).* Following the general procedure, 538 mg of 4-trifluoromethyl-2-bromobenzoic acid (**13f**; 2.0 mmol) gave 336 mg (1.0 mmol) of oxazoline **15f** as a clear oil (50%). Data for the amide are as follows. ^{1}H NMR (400 MHz, $CDCl_3$): δ 7.85 (s, 1 H), 7.61 (s, 2 H), 6.34 (d, J = 8.4 Hz, 1 H), 3.95 (m, 1 H), 3.80 (m, 2 H), 2.50 (bs, 1 H), 2.0 (m, 1 H), 1.05 (d, J = 6.8 Hz, 3 H), 1.04 (d, J = 6.8 Hz, 3 H). Data for the oxazoline are as follows: $[\alpha]_D$ = −41.0° (*c* 2.05, $CHCl_3$). ^{1}H NMR (400 MHz, $CDCl_3$): δ 7.9 (s, 1 H), 7.8 (d, J = 8.1 Hz, 1 H), 7.6 (dd, J = 8.1, 0.6 Hz, 1 H), 4.4 (m, 1 H), 4.2 (m, 2 H), 1.9 (m, 1 H), 1.05 (d, J = 6.8 Hz, 3 H), 1.00 (d, J = 6.8 Hz, 3 H). $^{13}C\{^1H\}$ NMR

dx.doi.org/10.1021/om3007163 | *Organometallics* 2012, 31, 6933–6946

(100 MHz, $CDCl_3$): δ 161.7, 133.6, 133.2 (q, J = 33 Hz), 131.7, 130.7 (q, J = 4 Hz), 123.9 (q, J = 4 Hz), 122.8 (q, J = 273 Hz), 122.2, 73.1, 70.6, 32.6, 18.6, 18.2. IR (neat): 2961, 1656, 1318, 1130 cm^{-1}. Anal. Calcd for $C_{13}H_{13}BrF_3NO$: C, 46.45; H, 3.90; N, 4.17. Found: C, 46.46; H, 3.83; N, 4.25.

*(−)-(4S)-4,5-Dihydro-2-(5′-(dimethylamino)-2′-bromophenyl)-4-isopropyloxazole (**16a**).* Following the general procedure, 473 mg of 5-dimethylamino-2-bromobenzoic acid (**14a**; 1.95 mmol) gave 299 mg (41%) of oxazoline **16a** as a clear/yellow oil. Data for the amide are as follows. ^1H NMR (400 MHz, $CDCl_3$): δ 7.3 (d, J = 8.9 Hz, 1 H), 6.8 (d, J = 3.1 Hz, 1 H), 6.5 (dd, J = 8.9, 3.1 Hz, 1 H), 6.4 (d, J = 8.6 Hz, 1 H), 3.9 (m, 1 H), 3.7 (m, 1 H), 3.1 (bs, 1 H), 2.9 (s, 6 H), 2.0 (m, 1 H), 1.0 (d, J = 6.8 Hz, 3 H), 0.98 (d, J = 6.8 Hz, 3 H). Data for the oxazoline are as follows. $[\alpha]_D$ = −34.5° (*c* 2.13, $CHCl_3$). ^1H NMR (400 MHz, $CDCl_3$): δ 7.3 (d, J = 9.0 Hz, 1 H), 6.9 (d, J = 3.1 Hz, 1 H), 6.5 (dd, J = 8.9, 3.1 Hz, 1 H), 4.3 (m, 1 H), 4.1 (m, 2 H), 2.9 (s, 6 H), 1.85 (m, 1 H), 1.0 (d, J = 6.8 Hz, 3 H), 0.95 (d, J = 6.8 Hz, 3 H). $^{13}C\{^1H\}$ NMR (100 MHz, $CDCl_3$): δ 163.2, 145.0, 133.5, 129.8, 115.2, 114.4, 106.9, 72.6, 69.9, 40.1, 32.4, 18.6, 18.0. IR (neat): 2958, 1594, 1491, 1362, 1226, 1172, 1109, 1012, 973, 729 cm^{-1}. Anal. Calcd for $C_{14}H_{19}BrN_2O$: C, 54.03; H, 6.15; N, 9.00. Found: C, 53.99; H, 6.27; N, 8.92.

*(−)-(4S)-4,5-Dihydro-2-(5′-fluoro-2′-bromophenyl)-4-isopropyloxazole (**16d**).* Following the general procedure, 657 mg of 5-fluoro-2-bromobenzoic acid (**14d**; 3.0 mmol) gave 638 mg (74%) of oxazoline **16d** as a clear oil. Data for the amide are as follows. ^1H NMR (400 MHz, $CDCl_3$): δ 7.6 (dd, J = 8.8, 5.0 Hz, 1 H), 7.5 (dd, J = 8.4, 3.0 Hz, 1 H), 7.0 (ddd, J = 8.8, 3.0, 8.4 Hz, 1 H), 6.23 (m, 1 H), 4.0 (m, 1 H), 3.8 (m, 2 H), 2.1 (m, 1 H), 1.86 (bs, 1 H), 1.0 (d, J = 6.8 Hz, 6 H). Data for the oxazoline are as follows. $[\alpha]_D$ = −67.4° (*c* 1.45, $CHCl_3$). ^1H NMR (400 MHz, $CDCl_3$): δ 7.5−7.6 (dd, J = 8.8, 5.1 Hz, 1 H), 7.4 (dd, J = 8.8, 3.1 Hz, 1 H), 6.9−7.0 (ddd, J = 8.8, 8.8, 3.1 Hz, 1 H), 4.4 (m, 1 H), 4.1−4.2 (m, 2 H), 1.85 (m, 1 H), 1.0 (d, J = 6.8 Hz, 3 H), 0.93 (d, J = 6.8 Hz, 3 H). $^{13}C\{^1H\}$ NMR (100 MHz, $CDCl_3$): δ 161.6 (d, J = 2 Hz), 161.2 (d, J = 248 Hz), 135.1 (d, J = 8 Hz), 131.5 (d, J = 8 Hz), 118.7 (d, J = 22 Hz), 118.4 (d, J = 25 Hz), 116.0 (d, J = 3 Hz), 73.0, 70.4, 32.6, 18.6, 18.1. IR (neat): 2960, 2874, 2360, 1653 cm^{-1}. Anal. Calcd for $C_{12}H_{13}BrFNO$: C, 50.37; H, 4.58; N, 4.90. Found: C, 50.57; H, 4.43; N, 4.99.

*(−)-(4S)-4,5-Dihydro-2-(5′-(trifluoromethyl)-2′-bromophenyl)-4-isopropyloxazole (**16f**).* Following the general procedure, 1.08 g of 5-trifluoromethyl-2-bromobenzoic acid (**14f**) (4.0 mmol), gave 656 mg (49%) of oxazoline **16f** as a clear oil. Data for the amide are as follows. ^1H NMR (400 MHz, $CDCl_3$): δ 7.82 (d, J = 2.0 Hz, 1 H), 7.75 (d, J = 8.4 Hz, 1 H), 7.55 (dd, J = 8.4, 2.0 Hz, 1 H), 6.35 (bs, 1 H), 4.0 (m, 1 H), 3.85 (m, 2 H), 2.5 (bs, 1 H), 2.05 (m, 1 H), 1.08 (d, J = 6.8 Hz, 6 H). Data for the oxazoline are as follows. $[\alpha]_D$ = −50.4° (*c* 2.20, $CHCl_3$). ^1H NMR (400 MHz, $CDCl_3$): δ 7.95 (d, J = 1.8 Hz, 1 H), 7.76 (d, J = 8.4 Hz, 1 H), 7.5 (dd, J = 8.3, 2.0 Hz, 1 H), 4.45 (m, 1 H), 4.2 (m, 2 H), 1.9 (m, 1 H), 1.05 (d, J = 7.2 Hz, 3 H), 0.99 (d, J = 6.8 Hz, 3 H). $^{13}C\{^1H\}$ NMR (100 MHz, $CDCl_3$): δ 161.5, 134.5, 130.9, 129.4 (q, J = 34 Hz), 128.2 (q, J = 4 Hz), 127.9 (q, J = 4 Hz), 125.9 (m), 123.4 (q, J = 272 Hz), 73.1, 70.6, 32.6, 18.7, 18.2. IR (neat): 2961, 2906, 1657, 1698 cm^{-1}. Anal. Calcd for $C_{13}H_{13}BrF_3NO$: C, 46.45; H, 3.90; N, 4.17. Found: C, 46.34; H, 3.87; N, 4.34.

(−)-(4S)-4-Chloro-2-(4-isopropyl-4,5-dihydrooxazol-2-yl)-phenyl Trifluoromethanesulfonate (12e). In a 100 mL round-bottom flask was added 1.38 g of 5-chlorosalicylic acid (**11e**; 8 mmol, 1.0 equiv), 244 mg of 4-dimethylaminopyridine (2 mmol, 0.25 equiv), 991 mg of (*S*)-(+)-2-amino-3-methyl-1-butanol (9.6 mmol, 1.2 equiv), 50.0 mL of dichloromethane, and 1.84 g of 1-ethyl-3-(3-(dimethylamino)propyl)carbodiimide (9.6 mmol, 1.2 equiv). The reaction mixture was stirred at room temperature for 24 h. The solution was then cooled to −78 °C, and 3.68 g of triethylamine (40 mmol, 5 equiv; distilled) was added. Then, 6.05 g of trifluoromethanesulfonic anhydride (24 mmol, 3 equiv) was added dropwise via syringe over 15 min. After it was stirred for 2.5 h, the solution was transferred to a 0 °C ice bath before being warmed slowly to room temperature (the ice bath was allowed to melt) and subsequently heated to reflux for 12 h. After it was cooled to room temperature, the red reaction mixture was washed with 25 mL of water and 3 × 25 mL of saturated aqueous sodium bicarbonate. The organic layer was dried over anhydrous sodium sulfate and then concentrated in vacuo. Flash column chromatography (13 × 4.5 cm, 8% ethyl acetate in hexanes) gave 1.07 g (36%) of **12e** as a pale yellow oil. $[\alpha]_D$ = −35.4° (*c* 1.70, $CHCl_3$). ^1H NMR (400 MHz, $CDCl_3$): δ 8.0 (d, J = 2.5 Hz, 1 H), 7.5 (dd, J = 8.8, 2.8 Hz, 1 H), 7.24 (d, J = 8.8 Hz, 1 H), 4.45 (m, 1 H), 4.15 (m, 2 H), 1.9 (m, 1 H), 1.06 (d, J = 6.8 Hz, 3 H), 0.97 (d, J = 6.8 Hz, 3 H). $^{13}C\{^1H\}$ NMR (100 MHz, $CDCl_3$): δ 171.2, 158.7, 146.1, 134.1, 132.2, 131.6, 123.8, 119.1 (q, J = 239 Hz), 73.1, 70.6, 32.7, 18.8, 18.3. IR (neat): 2963, 1653, 1428, 1204, 1138, 875, 692 cm^{-1}. Anal. Calcd for $C_{13}H_{13}ClF_3NO_4S$: C, 42.00; H, 3.52; N, 3.77. Found: C, 42.29; H, 3.54; N, 3.63.

(−)-(4S)-4,5-Dihydro-2-(5′-methyl-2′-(diphenylphosphino)-phenyl)-4-isopropyloxazole (3c). In a 100 mL round-bottom flask was added 7.7 mL of anhydrous hexanes and 2.5 mL of 1.04 M *sec*-butyllithium in cyclohexane (2.4 mmol, 1.2 equiv). The solution was cooled to −78 °C, and 234 mg of *N*,*N*,*N*′,*N*′-tetramethylethylenediamine (2.2 mmol, 1.1 equiv) was added dropwise over 1−2 min. After the mixture was stirred for 10 min, a solution of 406 mg of **10c** (2.0 mmol, 1 equiv) in 1.0 mL of anhydrous hexanes was added dropwise via cannula over 5 min. The flask was rinsed with an additional 1.0 mL of anhydrous hexane, which was also added via cannula. The resulting dark red solution was stirred at −78 °C for 2 h. A solution of 883 mg of chlorodiphenylphosphine (4.0 mmol, 2 equiv) in 2.0 mL of anhydrous hexanes was then added dropwise via cannula over 5 min. The reaction mixture was stirred at −78 °C for 3 h before it was warmed to room temperature overnight. The reaction was quenched with 3.0 mL of dry silica gel added via syringe. The mixture was concentrated in vacuo to absorb the crude product onto the silica gel. Flash column chromatography (3 cm × 13 cm, 10% ethyl acetate in hexanes) gave 428 mg (55%) of the ligand as a oil/foam. $[\alpha]_D$ = −32.4° (*c* 2.61, $CHCl_3$). ^1H NMR (400 MHz, $CDCl_3$): δ 7.8 (m, 1H), 7.3 (m, 10 H), 7.1 (dq, J = 7.9, 0.7 Hz, 1 H), 6.8 (dd, J = 7.9, 4.1 Hz, 1 H), 4.2 (m, 1 H), 3.9 (m, 2 H), 2.4 (s, 3 H), 1.55 (m, 1 H), 0.86 (d, J = 6.7 Hz, 3 H), 0.75 (d, J = 6.7 Hz, 3 H). $^{13}C\{^1H\}$ NMR (100 MHz, $CDCl_3$): δ 163.2, 138.4 (d, J = 12 Hz), 138.2 (d, J = 10 Hz), 135.1 (d, J = 23 Hz), 134.2, 134.0, 133.9, 133.6 (d, J = 21 Hz), 131.2, 130.5 (d, J = 4 Hz), 128.4 (d, J = 8 Hz), 128.2, 128.1 (d, J = 11 Hz), 72.8, 70.0, 32.6, 20.8, 18.8, 18.3. $^{31}P\{^1H\}$ NMR (162 MHz, $CDCl_3$): δ −6.3. IR (neat): 2960, 1652 cm^{-1}. Anal. Calcd for $C_{25}H_{26}NOP$: C, 77.50; H, 6.76; N, 3.62. Found: C, 77.27; H, 6.93; N, 3.58.

(−)-(4S)-2-(5-Chloro-2-(diphenylphosphino)phenyl)-4-isopropyl-4,5-dihydrooxazole (3e). In a 25 mL round-bottom flask was added 750 mg of **12e** (2.02 mmol, 1.0 equiv) and 77.5 mg of dichlorobis(benzonitrile)palladium (0.20 mmol, 0.1 equiv), and the flask was purged/back-filled with argon three times before the addition of 5.0 mL of toluene (anhydrous). The solution was then heated to 110 °C, and 785 mg of (trimethylsilyl)diphenylphosphine (3.04 mmol, 1.5 equiv) was added, at which point the solution turned dark red. The reaction mixture was cooled to room temperature after 19 h and was then diluted with 10 mL of dichloromethane. The organic mixture was then washed with 10 mL of saturated aqueous sodium bicarbonate, 10 mL of water, and 10 mL of saturated aqueous sodium chloride before drying over anhydrous sodium sulfate. The solution was then filtered and concentrated in vacuo. Flash column chromatography (12 × 4.5 cm, 10% diethyl ether in hexanes) gave 339 mg (41%) of the ligand as a yellow oil. $[\alpha]_D$ = −34.2° (*c* 0.97, $CHCl_3$). ^1H NMR (400 MHz, $CDCl_3$): δ 7.95 (dd, J = 3.3, 2.5 Hz, 1 H), 7.32 (s, 10 H), 7.24 (dd, J = 8.3, 2.3 Hz, 1 H), 6.83 (dd, J = 8.3, 3.5 Hz, 1 H), 4.2 (m, 1 H), 3.9 (m, 2 H), 1.5 (m, 1 H), 0.83 (d, J = 6.8 Hz, 3 H), 0.73 (d, J = 6.8 Hz, 3 H). $^{13}C\{^1H\}$ NMR (100 MHz, $CDCl_3$): δ 161.8, 148.8, 137.8 (d, J = 27 Hz), 137.7 (d, J = 24 Hz), 135.3, 134.4, 134.1, 133.8, 133.6, 130.3, 129.8, 128.63 (d, J = 28 Hz), 128.50 (d, J = 11 Hz), 128.47 (d, J = 19 Hz), 73.3, 70.3, 32.8, 18.8, 18.4. $^{31}P\{^1H\}$ NMR (162 MHz, $CDCl_3$): δ −6.2. IR (in $CDCl_3$): 3069, 2958, 2928, 2903, 1762, 1654, 1547, 1464, 1434, 1349, 1239, 1206, 1144, 1080, 965 cm^{-1}. Anal. Calcd for $C_{24}H_{23}ClNOP$: C, 70.67; H, 5.68; N, 3.43. Found: C, 70.92; H, 5.86; 3.43.

dx.doi.org/10.1021/om3007163 | *Organometallics* 2012, 31, 6933−6946

General Procedure for Ligands 2f and 3a,b,d,f.[11c] A round-bottom Schlenk flask equipped with a glass stopcock valve, a glass stopper, and a stir bar was dried with a heat gun under vacuum and purged/back-filled with argon three times. After the flask was cooled to room temperature, copper(I) iodide (0.125 equiv), diphenylphosphine (1.88 equiv; distilled), *N*,*N*-dimethylethylenediamine (0.875 equiv), and toluene (0.25 M based on aryl bromide, anhydrous) were added. The solution was stirred at room temperature for 20 min. A solution of the aryl bromide (1.0 equiv) in toluene (0.25 M, anhydrous) was added to the mixture in the Schlenk flask, followed by the addition of solid cesium carbonate (3.75 equiv). The flask was sealed and the reaction mixture stirred at 110 °C for 6 h, initially forming a turbid bright yellow solution which gradually darkened until the mixture was dark red-brown. The reaction mixture was cooled to room temperature, and the solution was filtered through Celite, which was then rinsed with dichloromethane (3 × 10 mL). The combined organic phases were concentrated in vacuo. Complete removal of the toluene was necessary for clean chromatographic separation. Flash column chromatography (10% ethyl acetate in hexanes) gave the ligand.

*(−)-(4S)-4,5-Dihydro-2-(5′-methoxy-2′-(diphenylphosphino)-phenyl)-4-isopropyloxazole (**3b**).* A 50 mL round-bottom Schlenk flask equipped with a glass stopcock valve, a glass stopper, and a stir bar was dried with a heat gun under vacuum and purged/back-filled with argon three times. After the flask was cooled to room temperature, 23.8 mg of copper(I) iodide (0.125 mmol, 0.125 equiv), 350 mg of diphenylphosphine (1.88 mmol, 1.88 equiv, distilled), 77.1 mg of *N*,*N*-dimethylethylenediamine (0.875 mmol, 0.875 equiv), and 4.0 mL of toluene (anhydrous) were added. The solution was stirred at room temperature for 20 min. A solution of 298 mg of **16b** (1.0 mmol, 1.0 equiv) in 4.0 mL of toluene (anhydrous) was added to the mixture in the Schlenk flask, followed by the addition of 1.22 g of cesium carbonate (3.75 mmol, 3.75 equiv). The flask was sealed and the reaction mixture stirred at 110 °C for 6 h, initially forming a turbid bright yellow solution which gradually darkened until the mixture was dark red-brown. The reaction mixture was cooled to room temperature, and the solution was filtered through Celite, which was then rinsed with dichloromethane (3 × 10 mL). The combined organic phases were concentrated in vacuo. Flash column chromatography (1.5 cm × 12.5 cm, 10% ethyl acetate in hexanes) gave 278 mg (69%) of the ligand as a white solid. Mp: 78−79 °C. $[\alpha]_D = -31.2°$ (*c* 1.88, $CHCl_3$). ^1H NMR (400 MHz, $CDCl_3$): δ 7.5 (m, 1 H), 7.25−7.4 (m, 10 H), 6.88 (dd, *J* = 8.6, 2.6 Hz, 1 H), 6.81 (dd, *J* = 8.6, 3.5 Hz, 1 H), 4.2 (m, 1 H), 3.95 (m, 2 H), 3.85 (s, 3 H), 1.6 (m, 1 H), 0.85 (d, *J* = 6.7 Hz, 3 H), 0.76 (d, *J* = 6.7 Hz, 3 H). $^{13}C\{^1H\}$ NMR (100 MHz, $CDCl_3$): δ 162.8 (d, *J* = 3 Hz), 159.1, 138.9 (d, *J* = 13 Hz), 138.7 (d, *J* = 11 Hz), 135.6, 134.2 (d, *J* = 21 Hz), 133.6 (d, *J* = 20 Hz), 133.5 (d, *J* = 22 Hz), 129.4 (d, *J* = 22 Hz), 128.3 (d, *J* = 20 Hz), 128.3 (d, *J* = 5 Hz), 116.6, 115.0 (d, *J* = 4 Hz), 73.2, 70.2, 55.4, 32.8, 18.9, 18.5. $^{31}P\{^1H\}$ NMR (162 MHz, $CDCl_3$): δ −7.54. IR (solid): 3052, 2957, 1652, 1593, 1222, 1091, 731 cm^{-1}. Anal. Calcd for $C_{25}H_{26}PNO_2$: C, 74.42; H, 6.50; N, 3.47. Found: C, 74.32; H, 6.58; N, 3.55.

*(−)-(4S)-4,5-Dihydro-2-(4′-trifluoromethyl-2′-(diphenylphosphino)phenyl)-4-isopropyloxazole (**2f**).* Following the general procedure, 253 mg of **15f** (0.75 mmol) gave 207 mg (63%) of **2f** as a faint yellow oil. $[\alpha]_D = -22.0°$ (*c* 1.34, $CHCl_3$). ^1H NMR (400 MHz, $CDCl_3$): δ 8.05 (dd, *J* = 8.0 Hz, 3.3 Hz, 1 H), 7.6 (d, *J* = 8.1 Hz, 1 H), 7.2−7.4 (m, 10 H), 7.15 (s, 1 H), 4.2 (m, 1 H), 3.9 (m, 2 H), 1.5 (m, 1 H), 0.85 (d, *J* = 6.7 Hz, 3 H), 0.75 (d, *J* = 6.7 Hz, 3 H). $^{13}C\{^1H\}$ NMR (100 MHz, $CDCl_3$): δ 161.8 (d, *J* = 3 Hz), 140.9 (d, *J* = 30 Hz), 137.2 (d, *J* = 19 Hz), 137.1 (d, *J* = 17 Hz), 134.9 (d, *J* = 18 Hz), 134.1 (d, *J* = 21 Hz), 133.6 (d, *J* = 21 Hz), 131.9 (q, *J* = 32 Hz), 130.3 (dq, *J* = 2, 2 Hz), 130.1 (d, *J* = 2 Hz), 128.8 (d, *J* = 23 Hz), 128.55 (d, *J* = 7 Hz), 128.5, 128.4, 124.6 (q, *J* = 3 Hz), 123.6 (q, *J* = 273 Hz), 73.3, 70.25, 32.7, 18.8, 18.3. $^{31}P\{^1H\}$ NMR (162 MHz, $CDCl_3$): δ −4.6. IR (neat): 3209, 2959, 1652, 1320, 1127, 734, 695 cm^{-1}. Anal. Calcd for $C_{25}H_{23}F_3NOP$: C, 68.02; H, 5.25; N, 3.17. Found: C, 68.04; H, 5.19; N, 3.30.

*(−)-(4S)-4,5-Dihydro-2-(5′-(dimethylamino)-2′-(diphenylphosphino)phenyl)-4-isopropyloxazole (**3a**).* Following the general procedure, 190 mg of **16a** (0.61 mmol) gave 128 mg (50%) of **3a** as a white solid. Mp: 128 °C. $[\alpha]_D = -33.8°$ (*c* 1.70, $CHCl_3$). ^1H NMR (400 MHz, $CDCl_3$): δ 7.2−7.3 (m, 10 H), 6.8 (dd, *J* = 8.6, 4.1 Hz, 1 H), 6.7 (dd, *J* = 8.6, 2.8 Hz, 1 H), 4.2 (m, 1 H), 3.9 (m, 2 H), 3.0 (s, 6 H), 1.6 (m, 1 H), 0.85 (d, *J* = 6.7 Hz, 3 H), 0.77 (d, *J* = 6.7 Hz, 3 H). $^{13}C\{^1H\}$ NMR (100 MHz, $CDCl_3$): δ 163.7, 145.0, 139.4 (d, *J* = 18 Hz), 139.3 (d, *J* = 15 Hz), 135.3, 134.1, 133.9, 133.5, 133.4, 128.1 (d, *J* = 18 Hz), 128.05 (d, *J* = 11 Hz), 127.95 (d, *J* = 21 Hz), 122.8 (d, *J* = 18 Hz), 114.0, 113.3 (d, *J* = 4 Hz), 73.0, 70.0, 40.1, 32.8, 18.8, 18.4. $^{31}P\{^1H\}$ NMR (162 MHz, $CDCl_3$): δ −8.38. IR (solid): 2868, 1596, 1431, 1182, 1028, 857 cm^{-1}. Anal. Calcd for $C_{26}H_{29}PN_2O$: C, 74.98; H, 7.02; N, 6.73. Found: C, 74.91; H, 7.05; N, 6.58.

*(−)-(4S)-4,5-Dihydro-2-(5′-fluoro-2′-(diphenylphosphino)-phenyl)-4-isopropyloxazole (**3d**).* Following the general procedure, 377 mg of **16d** (1.32 mmol) gave 302 mg (58%) of **3d** as a clear oil. $[\alpha]_D = -40.3°$ (*c* 1.08, $CHCl_3$). ^1H NMR (400 MHz, $CDCl_3$): δ 7.6−7.7 (d, *J* = 9.5, 2.8 Hz, 1 H), 7.25−7.4 (m, 10 H), 7.0 (d, *J* = 8.4, 2.8 Hz, 1 H), 6.8−6.9 (ddd, *J* = 9.0, 5.9, 3.4 Hz, 1 H), 4.2 (m, 1 H), 3.85−4.0 (m, 2 H), 1.55 (m, 1 H), 0.85 (d, *J* = 6.7 Hz, 3 H), 0.75 (d, *J* = 6.7 Hz, 3 H). $^{13}C\{^1H\}$ NMR (100 MHz, $CDCl_3$): δ 162.3 (d, *J* = 249 Hz), 161.7 (d *J* = 3 Hz), 138.2 (d, *J* = 13 Hz), 137.9 (d, *J* = 10 Hz), 136.0 (d, *J* = 8 Hz), 134.5 (d, *J* = 4 Hz), 134.3, 134.2, 134.1 (d, *J* = 21 Hz), 134.0, 133.9, 133.7 (d, *J* = 8 Hz), 133.5 (d, *J* = 20 Hz), 128.6, 128.5, 128.4, 128.33, 128.26, 117.3 (d, *J* = 20 Hz), 116.9 (d, *J* = 23 Hz), 73.2, 70.2, 32.7, 18.6, 18.4. $^{31}P\{^1H\}$ NMR (162 MHz, $CDCl_3$): δ −6.8. IR (neat): 3069, 2958, 2872, 2360, 1653 cm^{-1}. Anal. Calcd for $C_{24}H_{23}PFNO$: C, 73.64; H, 5.92; N, 3.58. Found: C, 73.57; H, 6.09; N, 3.55.

*(−)-(4S)-4,5-Dihydro-2-(5′-(trifluoromethyl)-2′-(diphenylphosphino)phenyl)-4-isopropyloxazole (**3f**).* Following the general procedure, 443 mg of **16f** (1.31 mmol) gave 309 mg (54%) of **3f** as a clear oil. $[\alpha]_D = -27.9°$ (*c* 1.2, $CHCl_3$). ^1H NMR (400 MHz, $CDCl_3$): δ 8.23 (s, 1 H), 7.54 (d, *J* = 8.1 Hz, 1 H), 7.3−7.5 (m, 10 H), 7.0 (dd, *J* = 8.0, 3.5 Hz, 1 H), 4.25 (m, 1 H), 3.9 (m, 2 H), 1.55 (m, 1 H), 0.84 (d, *J* = 6.7 Hz, 3 H), 0.73 (d, *J* = 6.7 Hz, 3 H). $^{13}C\{^1H\}$ NMR (100 MHz, $CDCl_3$): δ 161.6 (d, *J* = 4 Hz), 144.2 (d, *J* = 30 Hz), 137.5 (d, *J* = 12 Hz), 137.1 (d, *J* = 9 Hz), 134.3 (d, *J* = 2 Hz), 134.2 (d, *J* = 21 Hz), 133.6 (d, *J* = 21 Hz), 132.6 (d, *J* = 21 Hz), 132.2 (d, *J* = 18 Hz), 130.1 (q, *J* = 33 Hz), 128.8 (d, *J* = 21 Hz), 128.5 (d, *J* = 7 Hz), 128.4 (d, *J* = 8 Hz), 126.4 (m), 123.7 (q, *J* = 272 Hz), 73.3, 70.2, 32.7, 18.8, 18.3. $^{31}P\{^1H\}$ NMR (162 MHz, $CDCl_3$): δ −4.6. IR (neat): 3072, 2961, 1654, 1479, 1434, 1406, 1355 cm^{-1}. Anal. Calcd for $C_{25}H_{23}F_3NOP$: C, 68.02; H, 5.25; N, 3.17. Found: C, 68.28; H, 5.18; N, 3.24.

General Procedure for Complexes 5f and 6a−f.[15b] To a 10 mL round-bottom flask was added silver tetrafluoroborate (1.05 equiv), bis(μ-chloro)bis(1,3-diphenyl-η^3-allyl)dipalladium (0.525 equiv), and acetone (0.33 M based on ligand; distilled and degassed). The resulting solution was stirred in the dark under nitrogen for 1 h. The solution was then filtered through Celite in a sintered-glass funnel into a 10 mL round-bottom flask containing the ligand (1.0 equiv) and stirred overnight under nitrogen. The solvent was then removed in vacuo to give the product as a yellow to orange solid in quantitative yield suitable for NMR studies as an 8/1 to 9/1 mixture of exo/endo diastereomers, as measured by integration of the allyl H-3 signal at δ 5.8−6.0 ppm (exo) and δ 5.5−5.7 ppm (endo) in the ^1H NMR.

*(1,3-Diphenyl-η^3-allyl)((−)-(4S)-4,5-dihydro-2-(5′-methoxy-2′-(diphenylphosphino)phenyl)-4-isopropyloxazole)palladium(II) Tetrafluoroborate (**6b**).* In a 10 mL round-bottom flask was added 16.9 mg of silver tetrafluoroborate (0.087 mmol, 1.05 equiv), 29.1 mg of bis(μ-chloro)bis(1,3-diphenyl-η^3-allyl)dipalladium (0.043 mmol, 0.525 equiv), and 249 μL of acetone (distilled and degassed). The resulting solution was stirred in the dark under nitrogen for 1 h. The solution was then filtered through Celite in a sintered-glass funnel into a 10 mL round-bottom flask containing 33.4 mg of **3b** (0.083 mmol, 1.0 equiv) and stirred overnight under nitrogen. The solvent was then removed in vacuo to give complex **6b** as a yellow solid in quantitative yield suitable for NMR studies as a 91/9 mixture of exo/endo diastereomers, as measured by integration of the allyl H-3 signal at δ 5.87 ppm (exo) and δ 5.54 ppm (endo) in the ^1H NMR. The product

dx.doi.org/10.1021/om3007163 | *Organometallics* 2012, 31, 6933−6946

was purified for analysis by repeated washes with diethyl ether. Data for the exo diastereomer are as follows. ^{1}H NMR (400 MHz, CD_2Cl_2): δ 6.8−7.8 (m, 24 H), 5.87 (dd, J = 13.8, 9.2 Hz, 1 H), 4.31 (d, J = 10.9 Hz, 1 H), 4.1 (m, 2 H), 3.88 (s, 3 H), 3.15 (m, 1 H), 1.5 (m, 1 H), 0.30 (d, J = 6.9 Hz, 3 H), 0.01 (d, J = 6.8 Hz, 3 H). ^{13}C{^{1}H} NMR (100 MHz, CD_2Cl_2): δ 164.7, 111.68 (allyl C-2), 100.92 (allyl C-3), 70.70 (allyl C-1), 69.8, 69.0, 56.4, 31.7, 18.2, 13.9. ^{31}P{^{1}H} NMR (162 MHz, CD_2Cl_2): δ 19.7. Data for the endo diastereomer are as follows. ^{1}H NMR (400 MHz, CD_2Cl_2): δ 6.8−7.8 (m, 22 H), 6.60 (t, J = 12.4 Hz, 1 H), 6.44 (dd, J = 12.0, 7.7 Hz, 1 H), 5.54 (t, J = 11.4 Hz, 1 H), 5.00 (d, J = 12.2 Hz, 1 H), 3.9 (m, 1 H), 3.84 (s, 3 H), 3.7 (m, 1 H), 3.45 (m, 1 H), 1.9 (m, 1 H), 1.0 (d, J = 6.9 Hz, 3 H), 0.7 (d, J = 6.9 Hz, 3 H). ^{13}C{^{1}H} NMR (100 MHz, CD_2Cl_2): δ 164.5, 111.22 (allyl C-2), 95.43 (allyl C-3), 74.61 (allyl C-1), 69.8, 68.5, 56.4, 31.9, 18.63, 13.2. ^{31}P{^{1}H} NMR (162 MHz, CD_2Cl_2): δ 24.20. HRMS: calcd for $C_{40}H_{39}BF_4NO_2PPd$ 702.1753, found 702.1756.

*(1,3-Diphenyl-η^3-allyl){(−)-(4S)-4,5-dihydro-2-(4′-trifluoromethyl-2′-diphenylphosphinophenyl)-4-isopropyloxazole}palladium(II) Tetrafluoroborate (**5f**).* Following the general procedure, complex **5f** was obtained as a yellow solid in quantitative yield suitable for NMR studies as an 89/11 mixture of exo/endo diastereomers, as measured by integration of the allyl H-3 signal at δ 5.98 ppm (exo) and δ 5.68 ppm (endo) in the ^{1}H NMR. The product was purified for analysis by repeated washes with diethyl ether. Data for the exo diastereomer are as follows. ^{1}H NMR (400 MHz, CD_2Cl_2): δ 6.8−8.4 (m, 24 H), 5.98 (dd, J = 13.8, 9.4 Hz, 1 H), 4.39 (d, J = 10.9 Hz, 1 H), 4.1−4.2 (m, 2 H), 3.15 (m, 1 H), 1.5−1.6 (m, 1 H), 0.3 (d, J = 6.9 Hz, 3 H), 0.0 (d, J = 6.9 Hz, 3 H). ^{13}C{^{1}H} NMR (100 MHz, CD_2Cl_2): δ 164.0, 111.93 (allyl C-2), 101.78 (allyl C-3), 71.85 (allyl C-1), 70.0, 69.3, 31.7, 18.3, 13.9. ^{31}P{^{1}H} NMR (162 MHz, CD_2Cl_2): δ 21.5. Data for the endo diastereomer are as follows. ^{1}H NMR (400 MHz, CD_2Cl_2): δ 6.8−8.4 (m, 22 H), 6.66 (t, J = 12.3 Hz, 1 H), 6.44 (dd, J = 11.9, 7.8 Hz, 1 H), 5.68 (t, J = 11.5 Hz, 1 H), 5.13 (d, J = 12.3 Hz, 1 H), 4.1−4.2 (m, 1 H), 3.95 (t, J = 9.7 Hz, 1 H), 3.55 (m, 1 H), 1.5−1.6 (m, 1 H), 0.87 (d, J = 6.9 Hz, 3 H), 0.70 (d, J = 6.9 Hz, 3 H). ^{13}C{^{1}H} NMR (100 MHz, CD_2Cl_2): δ 163.8, 111.44 (allyl C-2), 96.62 (allyl C-3), 75.82 (allyl C-1), 71.4, 68.9, 31.6, 18.8, 13.3. ^{31}P{^{1}H} NMR (162 MHz, CD_2Cl_2): δ 25.8. HRMS: calcd for $C_{40}H_{36}BF_7NOPPd$: 740.1521. Found: 740.1521.

*(1,3-Diphenyl-η^3-allyl){(−)-(4S)-4,5-dihydro-2-(5′-dimethylamino-2′-diphenylphosphinophenyl)-4-isopropyloxazole}palladium(II) Tetrafluoroborate (**6a**).* Following the general procedure, complex **6a** was obtained as an orange solid in quantitative yield suitable for NMR studies as a 90/10 mixture of exo/endo diastereomers as measured by integration of the allyl H-3 signal at δ 5.82 ppm (exo) and δ 5.47 ppm (endo) in the ^{1}H NMR. The product was purified for analysis by repeated washes with diethyl ether. Data for the exo diastereomer are as follows. ^{1}H NMR (400 MHz, CD_2Cl_2): δ 6.7−7.8 (m, 24 H), 5.82 (dd, J = 13.6, 9.2 Hz, 1 H), 4.24 (d, J = 10.7 Hz, 1 H), 4.1 (m, 2 H), 3.1 (m, 1 H), 3.04 (s, 6 H), 1.5 (m, 1H), 0.3 (d, J = 6.7 Hz, 3 H), 0.0 (d, J = 6.6 Hz, 3 H). ^{13}C{^{1}H} NMR (100 MHz, CD_2Cl_2): δ 165.5, 111.57 (allyl C-2), 100.39 (allyl C-3), 69.98 (allyl C-1), 69.7, 68.9, 40.2, 31.9, 18.2, 13.9. ^{31}P{^{1}H} NMR (162 MHz, CD_2Cl_2): δ 19.2. Data for the endo diastereomer are as follows. ^{1}H NMR (400 MHz, CD_2Cl_2): δ 6.7−7.8 (m, 22 H), 6.58 (t, J = 12.4 Hz, 1 H), 6.43 (dd, J = 11.6, 8.0 Hz, 1 H), 5.47 (t, J = 11.5 Hz, 1 H), 4.92 (d, J = 11.4 Hz, 1 H), 3.9 (t, J = 9.6 Hz, 1 H), 3.75 (m, 1 H), 3.45 (m, 1 H), 2.99 (s, 6 H), 1.7 (m, 1 H), 1.0 (d, J = 6.5 Hz, 3 H), 0.70 (d, J = 6.6 Hz, 3 H). ^{13}C{^{1}H} NMR (100 MHz, CD_2Cl_2): δ 165.4, 111.12 (allyl C-2), 94.85 (allyl C-3), 73.78 (allyl C-1), 69.7, 68.7, 40.3, 32.1, 18.6, 13.4. ^{31}P{^{1}H} NMR (162 MHz, CD_2Cl_2): δ 23.8. HRMS: calcd for $C_{41}H_{42}BF_4N_2OPPd$ 715.2070, found 715.2074.

*(1,3-Diphenyl-η^3-allyl){(−)-(4S)-4,5-dihydro-2-(5′-methyl-2′-diphenylphosphinophenyl)-4-isopropyloxazole}palladium(II) Tetrafluoroborate (**6c**).* Following the general procedure, complex **6c** was obtained as a yellow solid in quantitative yield suitable for NMR studies as a 90/10 mixture of exo/endo diastereomers, as measured by integration of the allyl H-3 signal at δ 5.89 ppm (exo) and δ 5.56 ppm (endo) in the ^{1}H NMR. The product was purified for analysis by recrystallization from acetonitrile by the slow vapor diffusion of diethyl ether. Data for the exo diastereomer are as follows. ^{1}H NMR (400 MHz, CD_2Cl_2): δ 6.7−8.2 (m, 24 H), 5.89 (dd, J = 13.8, 9.2 Hz, 1 H), 4.34 (d, J = 11.0 Hz, 1 H), 4.1 (m, 2 H), 3.15 (m, 1 H), 2.45 (s, 3 H), 1.5 (m, 1 H), 0.3 (d, J = 6.8 Hz, 3 H), 0.0 (d, J = 6.8 Hz, 3 H). ^{13}C{^{1}H} NMR (100 MHz, CD_2Cl_2): δ 165.0, 111.77 (allyl C-2), 101.03 (allyl C-3), 70.82 (allyl C-1), 69.7, 69.0, 31.7, 21.6 ($ArCH_3$), 18.2, 13.9. ^{31}P{^{1}H} NMR (162 MHz, CD_2Cl_2): δ 20.4. Data for the endo diastereomer are as follows. ^{1}H NMR (400 MHz, CD_2Cl_2): δ 6.7−8.2 (m, 22 H), 6.61 (t, J = 12.2 Hz, 1 H), 6.44 (dd, J = 11.8, 8.0 Hz, 1 H), 5.56 (t, J = 11.4 Hz, 1 H), 5.01 (d, J = 12.0 Hz, 1H), 3.85 (m, 1 H), 3.65 (m, 1 H), 3.45 (m, 1 H), 2.43 (s, 3 H), 1.7 (m, 1 H), 0.85 (d, J = 6.8 Hz, 3 H), 0.75 (d, J = 6.7 Hz, 3 H). ^{13}C{^{1}H} NMR (100 MHz, CD_2Cl_2): δ 164.9, 111.27 (allyl C-2), 95.48 (allyl C-3), 74.80 (allyl C-1), 69.7, 68.5, 31.9, 21.3 ($ArCH_3$), 17.6, 13.4. ^{31}P{^{1}H} NMR (162 MHz, CD_2Cl_2): δ 24.7. Anal. Calcd for $C_{40}H_{39}BF_4NOPPd$: C, 62.08; H, 5.08; N, 1.81. Found: C, 62.06; H, 5.09; N, 1.84.

*(1,3-Diphenyl-η^3-allyl){(−)-(4S)-4,5-dihydro-2-(5′-fluoro-2′-diphenylphosphinophenyl)-4-isopropyloxazole}palladium(II) Tetrafluoroborate (**6d**).* Following the general procedure, complex **6d** was obtained as a yellow-orange solid in quantitative yield suitable for NMR studies as an 87/13 mixture of exo/endo diastereomers, as measured by integration of the allyl H-3 signal at δ 5.95 ppm (exo) and δ 5.61 ppm (endo) in the ^{1}H NMR. For analysis, a foamy yellow solid formed upon washing with diethyl ether and evaporating solvent under high vacuum. Data for the exo diastereomer are as follows. ^{1}H NMR (400 MHz, CD_2Cl_2): δ 6.7−7.9 (m, 24 H), 5.95 (dd, J = 13.9, 9.4 Hz, 1 H), 4.38 (d, J = 10.9 Hz, 1 H), 4.1 (m, 2 H), 3.13 (m, 1 H), 1.5 (m, 1 H), 0.3 (d, J = 6.9 Hz, 3 H), 0.0 (d, J = 6.8 Hz, 3 H). ^{13}C{^{1}H} NMR (100 MHz, CD_2Cl_2): δ 163.8, 111.82 (allyl C-2), 101.53 (allyl C-3), 71.41 (allyl C-1),70.0, 69.1, 31.6, 18.1, 13.9. ^{31}P{^{1}H} NMR (162 MHz, CD_2Cl_2): δ 20.2. Data for the endo diastereomer are as follows. ^{1}H NMR (400 MHz, CD_2Cl_2): δ 6.7−7.9 (m, 22 H), 6.63 (t, J = 12.3 Hz, 1 H), 6.44 (dd, J = 12.0, 7.7 Hz, 1 H), 5.61 (t, J = 11.6 Hz, 1 H), 5.03 (d, J = 11.9 Hz, 1 H), 3.92 (t, J = 9.7 Hz, 1 H), 3.67 (m, 1 H), 3.45 (m, 1 H), 1.8 (m, 1 H), 0.87 (d, J = 7.2 Hz, 3 H), 0.70 (d, J = 6.9 Hz, 3 H). ^{13}C{^{1}H} NMR (100 MHz, CD_2Cl_2): δ 163.5, 111.38 (allyl C-2), 96.09 (allyl C-3), 75.41 (allyl C-1), 69.4, 68.7, 31.7, 18.6, 13.3. ^{31}P{^{1}H} NMR (162 MHz, CD_2Cl_2): δ 24.6. Anal. Calcd for $C_{39}H_{37}BF_5NOPPd$: C, 60.22; H, 4.66; N, 1.80. Found: C, 59.85; H, 4.82; N, 1.94.

*(1,3-Diphenyl-η^3-allyl){(−)-(4S)-4,5-dihydro-2-(5′-chloro-2′-diphenylphosphinophenyl)-4-isopropyloxazole}palladium(II) Tetrafluoroborate (**6e**).* Following the general procedure, complex **6e** was obtained as a yellow-brown solid in quantitative yield suitable for NMR studies as a 90/10 mixture of exo/endo diastereomers, as measured by integration of the allyl H-3 signal at δ 5.93 ppm (exo) and δ 5.59 ppm (endo) in the ^{1}H NMR. The product was purified for analysis by repeated washes with diethyl ether. Data for the exo diastereomer are as follows. ^{1}H NMR (400 MHz, CD_2Cl_2): 6.8−8.3 (m, 24 H), 5.93 (dd, J = 13.9, 9.3 Hz, 1 H), 4.38 (d, J = 10.9 Hz, 1 H), 4.1−4.2 (m, 2 H), 3.15 (m, 1 H), 1.5 (m, 1 H), 0.29 (d, J = 6.9 Hz, 3 H), 0.00 (d, J = 6.8 Hz, 3 H). ^{13}C{^{1}H} NMR (100 MHz, CD_2Cl_2): δ 164.0, 111.83 (allyl C-2), 101.64 (allyl C-3), 71.51 (allyl C-1),70.0, 69.9, 32.1, 18.2, 13.9. ^{31}P{^{1}H} NMR (162 MHz, CD_2Cl_2): δ 20.4. Data for the endo diastereomer are as follows. ^{1}H NMR (400 MHz, CD_2Cl_2): δ 6.8−8.3 (m, 22 H), 6.64 (t, J = 12.3 Hz, 1 H), 6.42 (dd, J = 11.9, 7.5 Hz, 1 H), 5.59 (t, J = 11.6 Hz, 1 H), 5.03 (t, J = 9.8 Hz, 1 H), 3.92 (t, J = 9.7 Hz, 1 H), 3.6 (m, 1 H), 3.4 (m, 1 H), 1.85 (m, 1 H), 0.87 (d, J = 6.9 Hz, 3 H), 0.68 (d, J = 7.0 Hz, 3 H).^{13}C{^{1}H} NMR (100 MHz, CD_2Cl_2): δ 163.5, 111.38 (allyl C-2), 96.09 (allyl C-3), 75.41 (allyl C-1), 69.2, 68.8, 31.9, 18.7, 13.3. ^{31}P{^{1}H} NMR (162 MHz, CD_2Cl_2): δ 27.9. HRMS: calcd for $C_{39}H_{36}BClF_4NOPPd$ 706.1258, found 706.1257.

*(1,3-Diphenyl-η^3-allyl){(−)-(4S)-4,5-dihydro-2-(5′-trifluoromethyl-2′-diphenylphosphinophenyl)-4-isopropyloxazole}palladium(II) Tetrafluoroborate (**6f**).* Following the general procedure, complex **6f** was obtained as a yellow solid in quantitative yield suitable for NMR studies as a 90/10 mixture of exo/endo diastereomers, as measured by integration of the allyl H-3 signal at δ 5.97 ppm (exo) and δ 5.65 ppm (endo) in the ^{1}H NMR. The product was purified for analysis by

dx.doi.org/10.1021/om3007163 | *Organometallics* 2012, 31, 6933−6946

repeated washes with diethyl ether. Data for the exo diastereomer are as follows. ^{1}H NMR (400 MHz, CD_2Cl_2): δ 6.8−8.4 (m, 24H), 5.97 (dd, J = 13.9, 9.3 Hz, 1H), 4.44 (d, J = 10.9 Hz, 1H), 4.1−4.2 (m, 2H), 3.15 (m, 1H), 1.55 (m, 1H), 0.3 (d, J = 6.9 Hz, 3H), 0.0 (d, J = 6.7 Hz, 3H). ^{13}C{^{1}H} NMR (100 MHz, CD_2Cl_2): δ 163.8, 111.93 (allyl C-2), 101.89 (allyl C-3), 71.92 (allyl C-1),70.0, 69.2, 31.6, 18.2, 13.8. ^{31}P{^{1}H} NMR (162 MHz, CD_2Cl_2): δ 21.2. Data for the endo diastereomer are as follows. ^{1}H NMR (400 MHz, CD_2Cl_2): δ 6.8−8.4 (m, 22H), 6.65 (t, J = 12.4 Hz, 1H), 6.44 (dd, J = 12.0, 7.5 Hz, 1H), 5.65 (t, J = 11.5 Hz, 1H), 5.12 (d, J = 12.3 Hz, 1H), 3.94 (t, J = 9.7 Hz, 1H), 3.76 (d, J = 13.1 Hz, 1H), 3.47 (m, 1H), 1.5 (m, 1H), 0.86 (d, J = 7.2 Hz, 3H), 0.70 (d, J = 6.9 Hz, 3H). ^{13}C{^{1}H} NMR (100 MHz, CD_2Cl_2): δ 163.6, 111.41 (allyl C-2), 96.39 (allyl C-3), 76.11 (allyl C-1), 71.3, 68.8, 31.7, 18.6, 13.2. ^{31}P{^{1}H} NMR (162 MHz, CD_2Cl_2): δ 25.5. Anal. Calcd for $C_{40}H_{36}BF_7NOPPd$: C, 58.03; H, 4.38; N, 1.69. Found: C, 57.66; H, 4.47; N, 1.92.

■ ASSOCIATED CONTENT

Supporting Information

Hammett plots without *m*-NMe_2 (Figures S1 and S2), separate Hammett plots for **5a−f** and **6a−f** versus σ_m or σ_p (Figures S3−S6), substituent constants used (Table S1), NMR data for **4** and **5a−e**, sample 2D and ^{13}C NMR spectra for **5d** (Figures S7−S9), and ^{1}H and ^{13}C NMR spectra of **4**, **5a−f**, and **6a−f**. This material is available free of charge via the Internet at http://pubs.acs.org.

■ AUTHOR INFORMATION

Corresponding Author

*E-mail: rbunt@middlebury.edu.

Notes

The authors declare no competing financial interest.

■ ACKNOWLEDGMENTS

We thank Research Corp., the donors of the Petroleum Research Fund, administered by the American Chemical Society, and the National Science Foundation (CHE-071451) for support of this research and we thank Prof. Sunhee Choi for helpful discussions of the data.

■ REFERENCES

(1) (a) Sprinz, J.; Helmchen, G. *Tetrahedron Lett.* **1993**, *34*, 1769−1772. (b) von Matt, P.; Pfaltz, A. *Angew. Chem., Int. Ed. Engl.* **1993**, *32*, 566−568. (c) Dawson, G. J.; Frost, C. G.; Williams, J. M. J.; Coote, S. J. *Tetrahedron Lett.* **1993**, *34*, 3149−3150.

(2) (a) Helmchen, G.; Pfaltz, A. *Acc. Chem. Res.* **2000**, *33*, 336−345. (b) Helmchen, G. *J. Organomet. Chem.* **1999**, *576*, 203−214. (c) Williams, J. M. J. *Synlett* **1996**, 705−710.

(3) For an overview see: *Transition Metal Catalyzed Enantioselective Allylic Substitution in Organic Synthesis*; Kazmaier, U., Ed.; Springer-Verlag: Berlin, 2012; Topics in Organometallic Chemistry *38*.

(4) For examples of PHOX ligands in other metal-catalyzed transformations see: (a) Petersen, K. S.; Stoltz, B. M. *Tetrahedron* **2011**, *67*, 4352−4357. (b) Franzke, A.; Voss, F.; Pfaltz, A. *Tetrahedron* **2011**, *67*, 4358−4363. (c) Wüstenberg, B.; Pfaltz, A. *Adv. Synth. Catal.* **2008**, *350*, 174−178. (d) Lu, Z.-L.; Neumann, E.; Pfaltz, A. *Eur. J. Org. Chem.* **2007**, 4189−4192. (e) Smidt, S. P.; Zimmermann, N.; Studer, M.; Pfaltz, A. *Chem. Eur. J.* **2004**, *10*, 4685−4693. (f) Cristina, G.-Y.; Janssen, J. P.; Rominger, F.; Helmchen, G. *Organometallics* **2004**, *23*, 5459−5470.

(5) Szabo, K. J. *Organometallics* **1996**, *15*, 1128−1133.

(6) (a) Goldfuss, B. *J. Organomet. Chem.* **2006**, *691*, 4508−4513. (b) Kollmar, M.; Steinhagen, H.; Janssen, J. P.; Goldfuss, B.; Malinovskaya, S. A.; Vázquez, J.; Rominger, F.; Helmchen, G. *Chem. Eur. J.* **2002**, *8*, 3103−3114. (c) Kollmar, M.; Goldfuss, B.; Reggelin, M.; Rominger, F.; Helmchen, G. *Chem. Eur. J.* **2001**, *7*, 4913−4927.

(7) (a) Junker, J.; Reif, B.; Junker, B.; Felli, I. C.; Reggelin, M.; Griesinger, C. *Chem. Eur. J.* **2000**, *6*, 3281−3286. (b) Steinhargen, H.; Reggelin, M.; Helmchen, G. *Angew. Chem., Int. Ed. Engl.* **1997**, *36*, 2108−2110.

(8) (a) Kleimark, J.; Johansson, C.; Olsson, S.; Hakansson, M.; Hansson, S.; Åkermark, B.; Norrby, P.-O. *Organometallics* **2011**, *30*, 230−238. (b) Widhalm, M.; Nettekoven, U.; Kalchhauser, H.; Mereiter, K.; Calhorda, M. J.; Felix, V. *Organometallics* **2002**, *21*, 315−325. (c) Adams, H.; Anderson, J. C.; Cubbon, R.; James, D. S.; Mathias, J. P. *J. Org. Chem.* **1999**, *64*, 8256−8262. (d) Blochl, P. E.; Tongi, A. *Organometallics* **1996**, *15*, 4125−4132.

(9) Constantine, R. N.; Kim, N.; Bunt, R. C. *Org. Lett.* **2003**, *5*, 2279−2282.

(10) Armstrong, P. B.; Bennett, L. M.; Constantine, R. N.; Fields, J. L.; Jasinski, J. P.; Staples, R. J.; Bunt, R. C. *Tetrahedron Lett.* **2005**, *46*, 1441−1445.

(11) (a) Bélanger, E.; Pouliot, M.-F.; Courtemanche, M.-A.; Paquin, J.-F. *J. Org. Chem.* **2012**, *77*, 317−331. (b) Nishimura, T.; Noishiki, A.; Hayashi, T. *Chem. Commun.* **2012**, *48*, 973−975. (c) McCougal, N. T.; Streuff, J.; Mukherjee, H.; Virgil, S. C.; Stoltz, B. M. *Tetrahedron Lett.* **2010**, *51*, 5550−5554. (d) Maxwell, A. C.; Flanagan, S. P.; Goddard, R.; Guiry, P. J. *Tetrahedron: Asymmetry* **2010**, *21*, 1458−1473. (e) Tani, K.; Behenna, D. C.; McFadden, R. M.; Stoltz, B. M. *Org. Lett.* **2007**, *9*, 2529−2533. (f) Flanagan, S. P.; Guiry, P. J. *J. Organomet. Chem.* **2006**, *691*, 2125−2154. (g) Busacca, C. A.; Grossbach, D.; Campbell, S. J.; Dong, Y.; Ericksson, M. C.; Harris, R. E.; Jones, P.-J.; Kim, J.-Y.; Lorenz, J. C.; McKellop, K. B.; O'Brien, E. M.; Qui, F.; Simpson, R. D.; Smith, L.; So, R. C.; Spinelli, E. M.; Vitous, J.; Zavattaro, C. *J. Org. Chem.* **2004**, *69*, 5187−5195. (h) RajanBabu, T. V.; Casalnuovo, A. L.; Ayers, T. A.; Nomura, N.; Jin, J.; Park, H.; Nandi, M. *Curr. Org. Chem.* **2003**, *7*, 301−316. (i) Saitoh, A.; Achiwa, K.; Tanaka, K.; Morimoto, T. *J. Org. Chem.* **2000**, *65*, 4227−4240.

(12) (a) Hansch, C.; Leo, A.; Taft, R. W. *Chem. Rev.* **1991**, *91*, 165−195. (b) Taft, R. W.; Topsom, R. D. *Prog. Phys. Org. Chem.* **1987**, *16*, 1−83. (c) Shorter, J. *Correlation Analysis of Organic Reactivity with Particular Reference to Multiple Regression*; Wiley: New York, 1982. (d) Swain, C. G.; Lupton, E. C. *J. Am. Chem. Soc.* **1968**, *90*, 4328−4337. (e) Hammett, L. P. *J. Am. Chem. Soc.* **1937**, *59*, 96−103.

(13) (a) Fristrup, P.; Tursky, M.; Madsen, R. *Org. Biomol. Chem.* **2012**, *10*, 2569−2577. (b) Harper, K. C.; Sigman, M. S. *Science* **2011**, *333*, 1875−1878. (c) Lane, D. R.; Beavers, C. M.; Olmstead, M. M.; Schore, N. E. *Organometallics* **2009**, *28*, 6789−6797. (d) Popeney, C.; Guan, Z. *Organometallics* **2005**, *24*, 1145−1155.

(14) (a) Tu, T.; Zhou, Y.-G.; Hou, X.-L.; Dai, L.-X.; Dong, X.-C.; Yu, Y.-H.; Sun, J. *Organometallics* **2003**, *22*, 1255−1265. (b) Macsari, I.; Hupe, E.; Szabo, K. J. *J. Org. Chem.* **1999**, *64*, 9547−9556. (c) von Matt, P.; Lloyd-Jones, G. C.; Minidis, A. B. E.; Pfaltz, A.; Macko, L.; Neuburger, M.; Zehnder, M.; Rüegger, H.; Pregosin, P. S. *Helv. Chim. Acta* **1995**, *78*, 265−284. (d) Åkermark, B.; Krakenbergen, B.; Hansson, S.; Vitagliano, A. *Organometallics* **1987**, *6*, 620−628.

(15) (a) Evstigneeva, E. M.; Flid, V. R. *Russ. Chem. Bull.* **2008**, *57*, 1194−1197. (b) Branchadell, V.; Moreno-Manas, M.; Pajuelo, F.; Pleixats, R. *Organometallics* **1999**, *18*, 4934−4941. (c) Moreno-Manas, M.; Pajuelo, F.; Parella, T.; Pleixats, R. *Organometallics* **1997**, *16*, 205−209. (d) Malet, R.; Moreno-Manas, M.; Parella, T.; Pleixats, R. *J. Org. Chem.* **1996**, *61*, 758−763.

(16) (a) Verma, R. P.; Hansch, C. *Chem. Rev.* **2001**, *111*, 2865−2899. (b) Lee, I.-S. H.; Jeon, H. J.; Yu, J. S.; Lee, C. K. *Bull. Korean Chem. Soc.* **2010**, *31*, 1689−1694. (c) Fröhlich, J.; Berger, S. *Eur. J. Org. Chem.* **2008**, 1632−1634. (d) Lin, S.-T.; Lee, C.-C.; Wu, E.-C. *Tetrahedron* **2008**, *64*, 5103−5106. (e) Lin, S.-T.; Lee, C.-C.; Lang, D. W. *Tetrahedron* **2000**, *56*, 9619−9623. (f) Tschoerner, M.; Kunz, R. W.; Pregosin, P. S. *Magn. Reson. Chem.* **1999**, *37*, 91−97.

(17) For examples of inverse Hammett correlations of ^{13}C NMR chemical shifts with hydrozones and imines due to π-polarization see: (a) Neuvonen, H.; Fülöp, F.; Neuvonen, K.; Kock, A.; Klenpeter, E. *J. Phys. Org. Chem.* **2008**, *21*, 173−184. (b) Neuvonen, H.; Neuvonen, K.; Fülöp, F. *J. Org. Chem.* **2006**, *71*, 3141.

(18) (a) Marinković, A. D.; Jovanović, B. Z.; Assaleh, F. H.; Vajs, V. V.; Juranić, M. I. *J. Mol. Struct.* **2012**, *1011*, 158−165. (b) Huang, S.; Wong, J. C. S.; Leung, A. K. C.; Chan, Y. M.; Ong, L.; Fernendez, M. R.; Miller, A. K.; Wu, W. *Tetrahedron Lett.* **2009**, *50*, 5018−5020. (c) Thirunarayanan, G.; Gopalakrishnan, M.; Vanangamudi, G. *Spectrochim. Acta, Part A* **2007**, *67*, 1106−1112. (d) Crisponi, G.; Casu, M.; Nurchi, V. M.; Cesare-Marincola, F.; Pivetta, T.; Silvagni, R. *Talanta* **2002**, *56*, 441−449. (e) Coulson, D. R. *J. Am. Chem. Soc.* **1976**, *98*, 3111−3119.
(19) Charton, M. *Prog. Phys. Org. Chem.* **1981**, *13*, 191−251.
(20) Hansch, C.; Leo, A.; Unger, S. H.; Kim, H. K.; Nikaitani, I.; Lien, E. J. *J. Med. Chem.* **1973**, *16*, 1207−1216.
(21) For a discussion of the trans effect by various ligating atoms in mixed donor chiral ligands, see ref 14a (and references therein).
(22) Koch, G.; Lloyd-Jones, G. C.; Loiseleur, O.; Pfaltz, A.; Pretot, R.; Schaffner, S.; Schnider, P.; von Matt, P. *Recl. Trav. Chim. Pays-Bas* **1995**, *114*, 206−210.
(23) Bald, E.; Saigo, K.; Mukaiyama, T. *Chem. Lett.* **1975**, 1163−1166.
(24) (a) Gant, T. G.; Meyers, A. I. *Tetrahedron* **1994**, *50*, 2297. (b) Peer, M.; de Jong, J. C.; Kiefer, M.; Langer, T.; Rieck, H.; Schell, H.; Sennhenn, P.; Sprintz, J.; Steinhagen, H.; Wiese, B.; Helmchen, G. *Tetrahedron* **1996**, *52*, 7547.
(25) Snieckus, V. *Chem. Rev.* **1990**, *90*, 879−933.
(26) (a) Ritter, K. *Synthesis* **1993**, 735−762. (b) Tunney, S. E.; Stille, J. K. *J. Org. Chem.* **1987**, *52*, 748−753.
(27) (a) Feng, J.; Bohle, D. S.; Li, C.-J. *Tetrahedron: Asymmetry* **2007**, *18*, 1043−1047. (b) Schwan, A. L. *Chem. Soc. Rev.* **2004**, *33*, 218−224. (c) Kwong, F. Y.; Lai, C. W.; Yu, M.; Tian, Y.; Chan, K. S. *Tetrahedron* **2003**, *59*, 10295−10305. (d) Kim, Y. K.; Lee, S. J.; Ahn, K. H. *J. Org. Chem.* **2000**, *65*, 7807−7813. (e) Ager, D. J.; East, M. B.; Eisenstdat, A.; Laneman, S. A. *Chem. Commun.* **1997**, 2359−2360. (f) Cai, D.; Payack, J. F.; Bender, D. R.; Hughes, D. L.; Verhoeven, T. R.; Reider, P. J. *J. Org. Chem.* **1994**, *59*, 7180−7181.
(28) Gelman, D.; Jiang, L.; Buchwald, S. L. *Org. Lett.* **2003**, *5*, 2315−2318.
(29) All the aryl bromides were commercially available except for **14a**, which was prepared by reductive methylation of 5-amino-2-bromobenzoic acid with CH_2O and $NaCNBH_3$; see: Ke-Qing Ling, K.-Q.; Sayre., L. M. *J. Org. Chem.* **2009**, *74*, 339−350.
(30) Sprinz, J.; Kiefer, M.; Helmchen, G.; Reggelin, M.; Huttner, G.; Walter, O.; Zsolnai, L. *Tetrahedron Lett.* **1994**, *35*, 1523−1526.
(31) The present data agree with all previously reported ^{13}C NMR data. In a few instances where very minor differences were observed (a few hundredths of a ppm), the most recent data are reported in this paper for consistency.
(32) For some examples see: (a) Mazuela, J.; Paptchikhine, A.; Tolstoy, P.; Pàmies, O.; Diéguez, M.; Andersson, P. G. *Chem. Eur. J.* **2010**, *16*, 620−638. (b) You, S. L.; Hou, X. L.; Dai, L. X.; Yu, Y. H.; Xia, W.; Sun, J. *J. Org. Chem.* **2002**, *67*, 4684−4695. (c) Dotta, P.; Kumar, P. G. A.; Pregosin, P. S. *Magn. Reson. Chem.* **2002**, *40*, 653−658. (d) Deng, W. P.; You, S. L.; Hou, X. L.; Dai, L. X.; Yu, Y. H.; Xia, W. *J. Am. Chem. Soc.* **2001**, *123*, 6508−6519.
(33) Baltzer, N.; Macko, L.; Schaffner, S.; Zehnder, M. *Helv. Chim. Acta* **1996**, *79*, 803−812.
(34) For an example of this type of analysis with a larger resonance component see: Lehmann, J.; Lloyd-Jones, G. C. *Tetrahedron* **1995**, *51*, 8863−8874.